DES Y3 results: Measurement of BAO with projected three-dimensional clustering

Kwan Chuen Chan （陈坤全）
Sun-Yat Sen University

In collaboration with Dark Energy Survey

SJTU, 19 Jun 2023

Dark Energy Survey Year 3

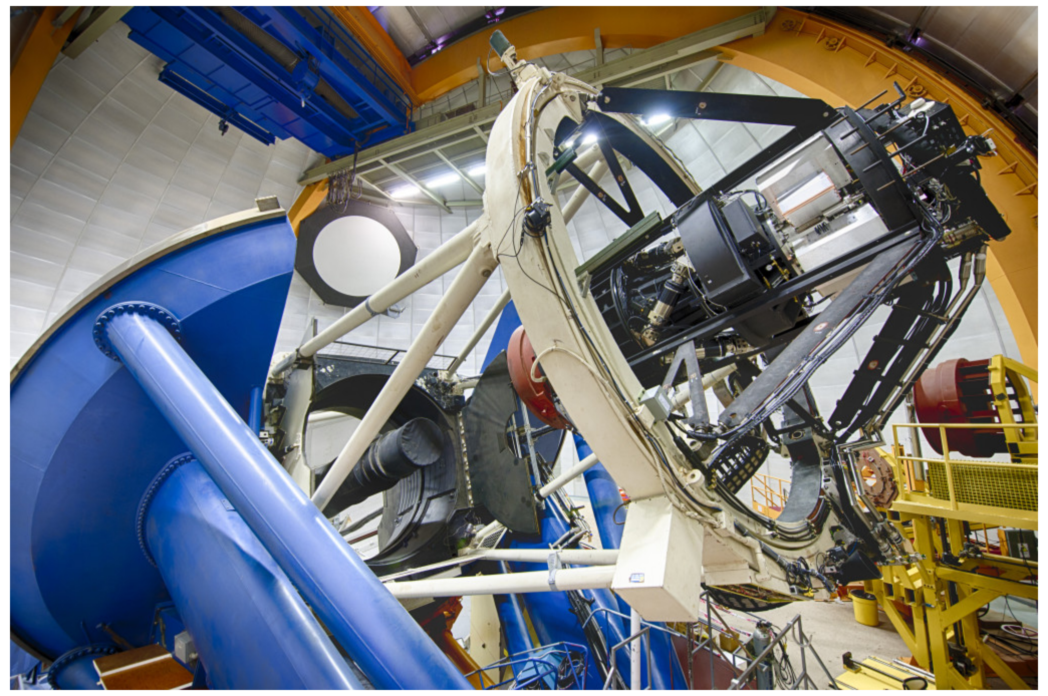

- Dark Energy Survey (DES) is an ongoing photometric survey, most well-known for weak lensing
- Blanco 4-meter telescope at Cerro Tololo Inter-American Observatory in Chile
- Dark Energy Camera, Field of view: 3 sq deg, 570-megapixels CCD
- Y3 observing time from 2013 to 2015

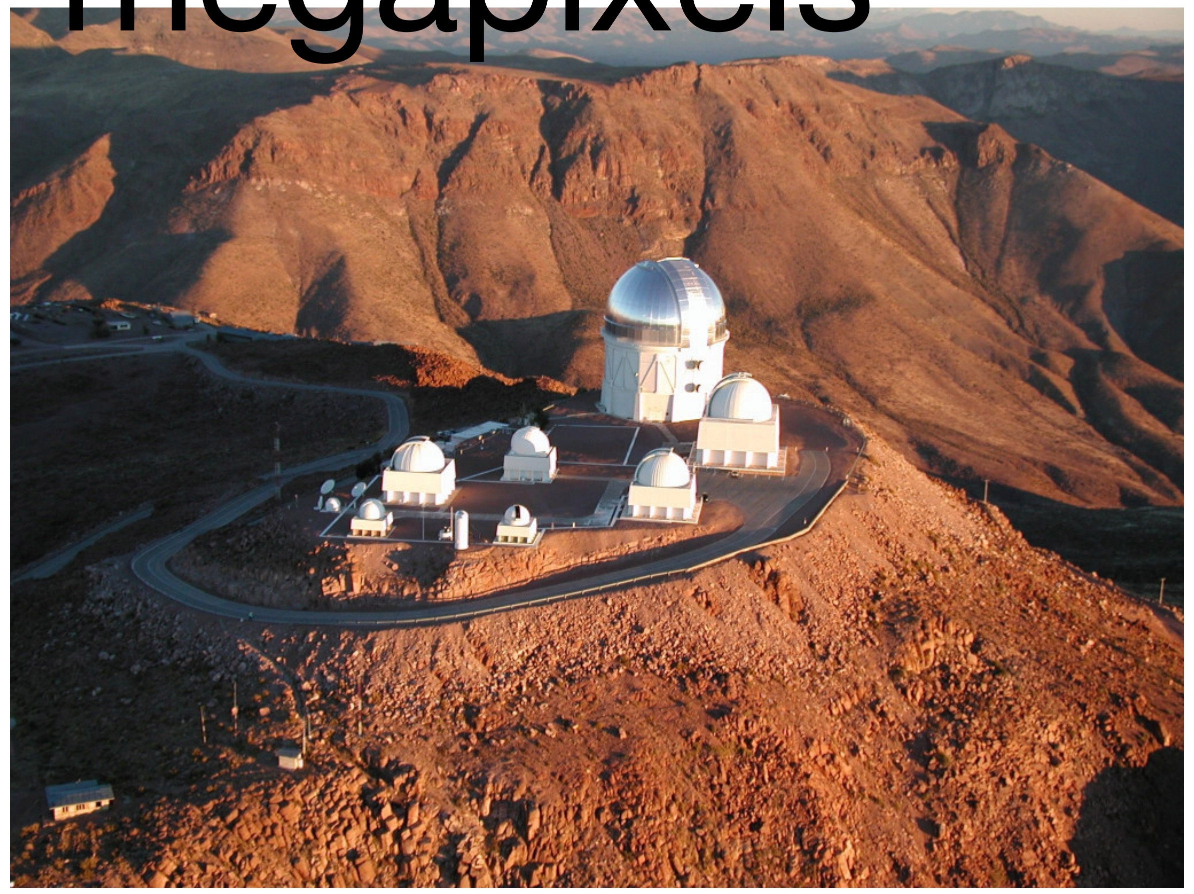

DES Y3

- DES Y3 gold sample covers about 5000 sq deg
- After masking, DES Y3 BAO sample covers about 4100 sq degree, with mean redshift of 0.83.

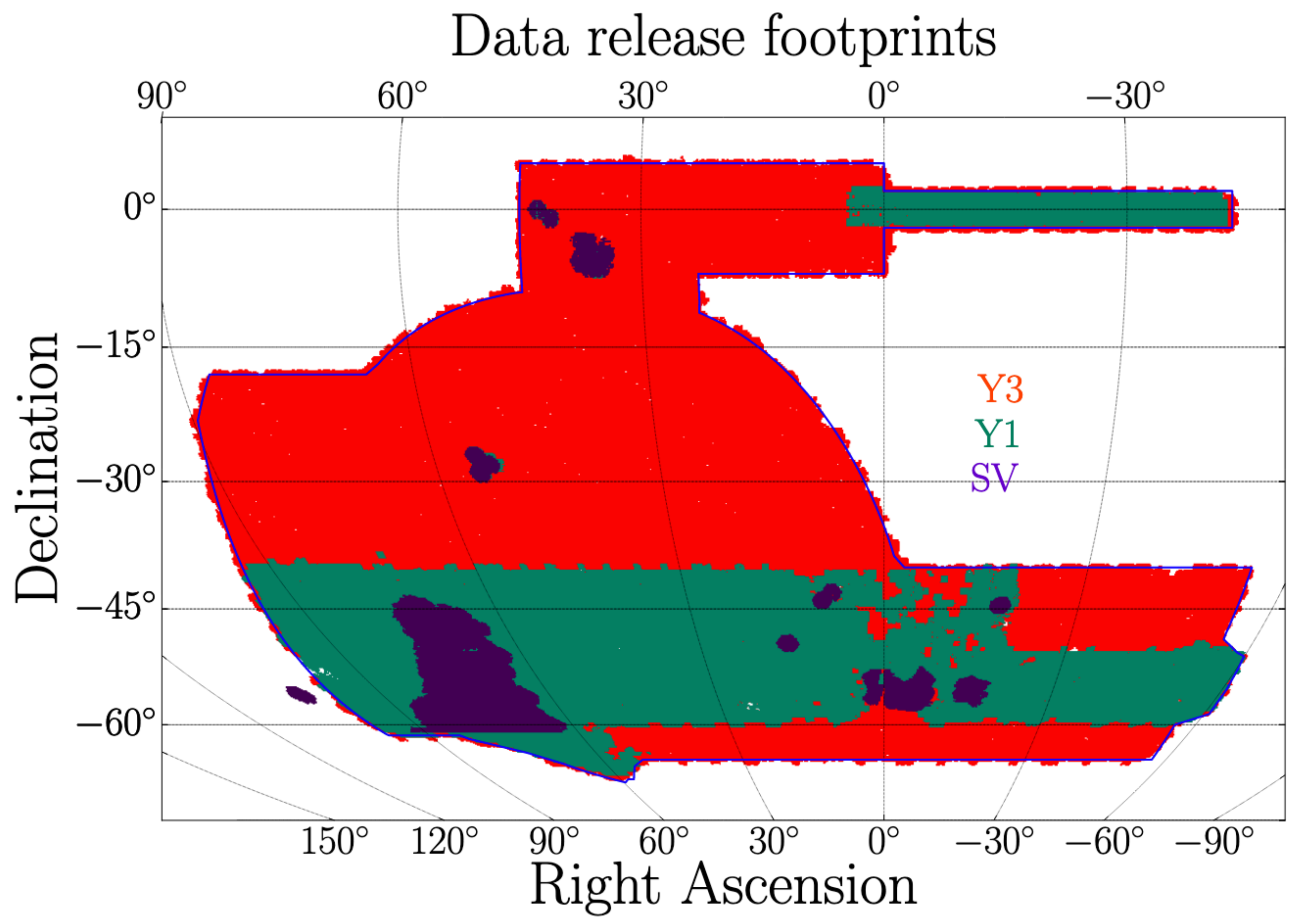

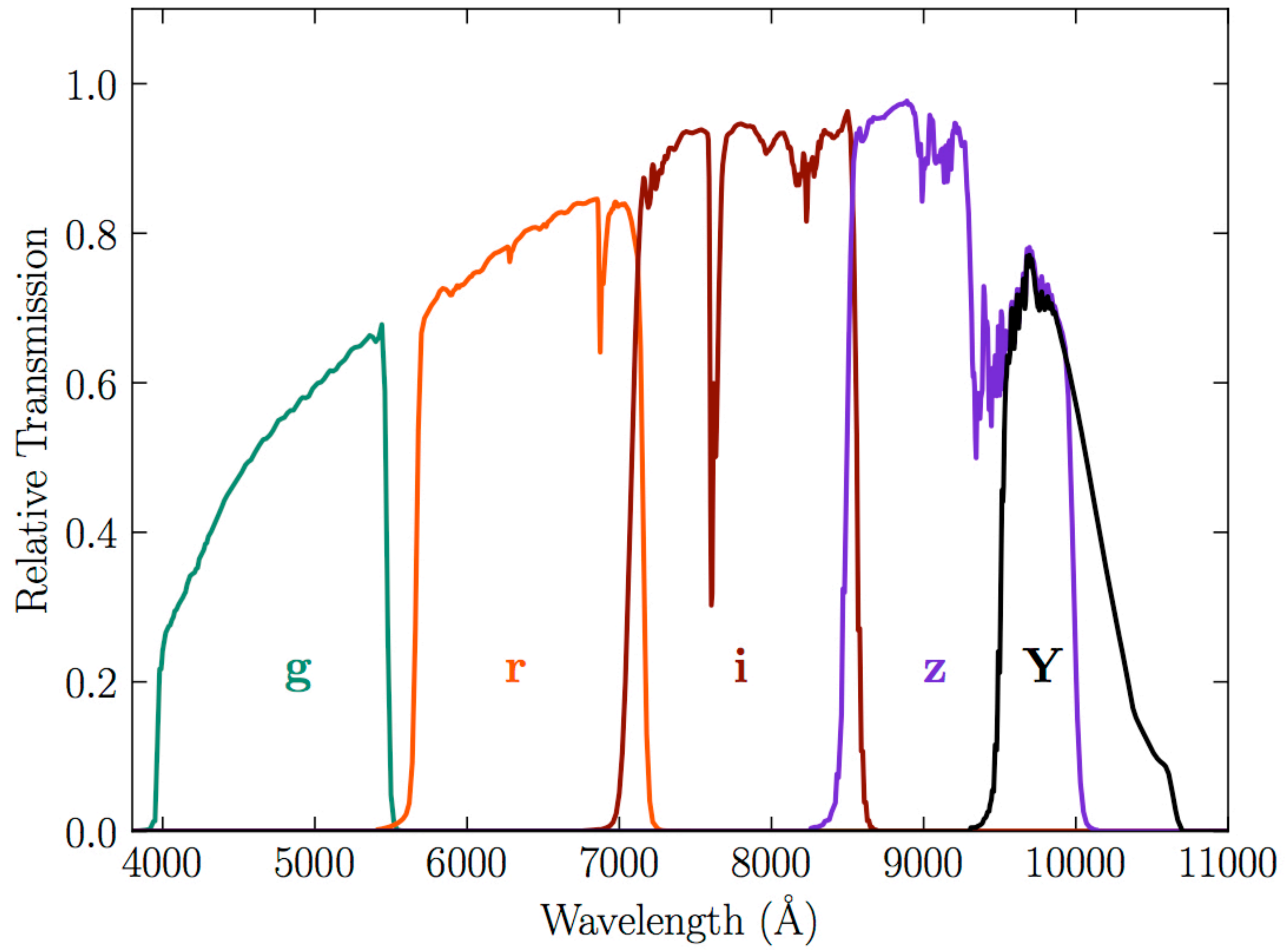

Sevilla-Noarbe +, 2011.03407

Baryonic Acoustic Oscillations (BAO)

- Acoustic oscillations during the early universe, imprinted in the distribution of the large-scale structure
- Standard ruler in the late universe
- Measured in numerous data analyses, mostly spec-z
- DES, lack of precise radial info, still preserve the transverse BAO.

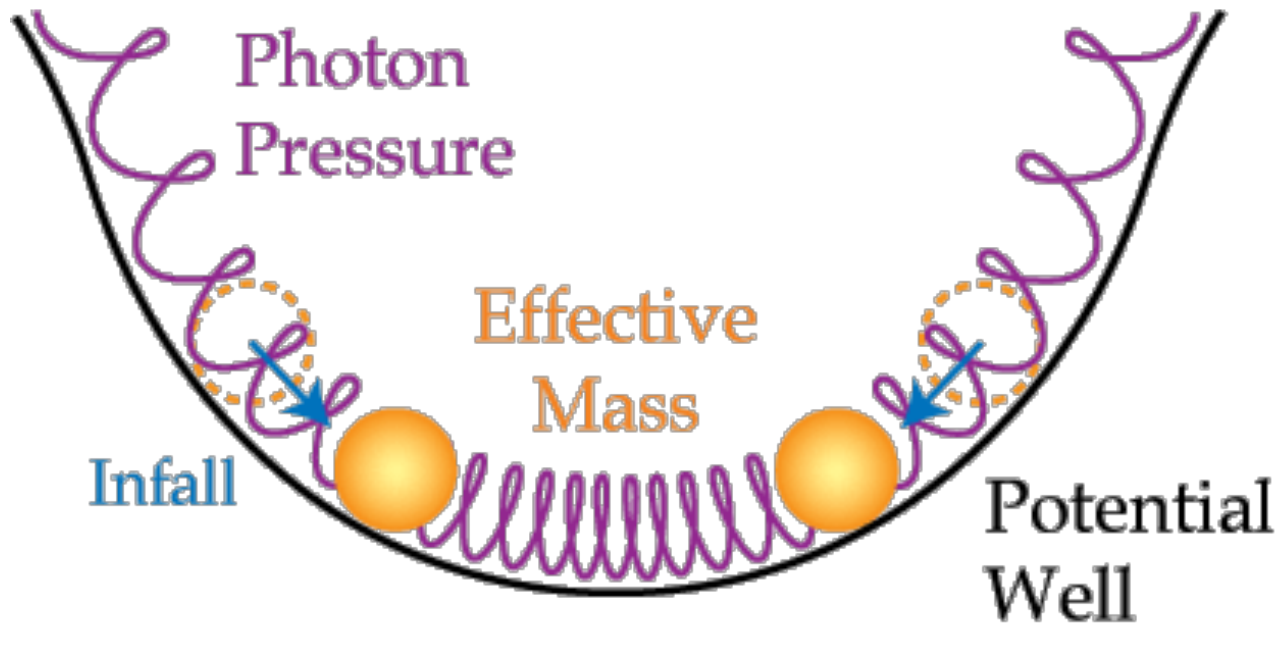

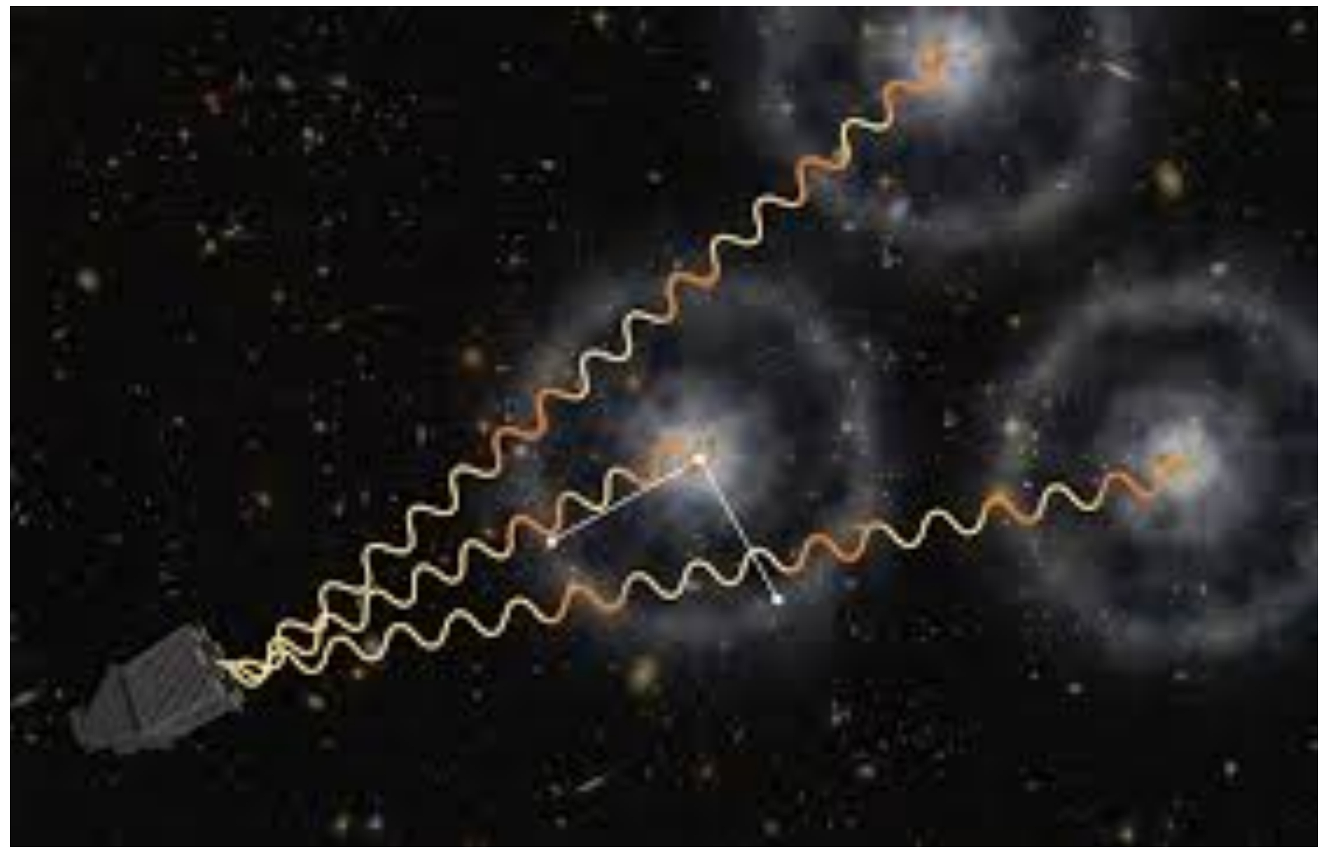

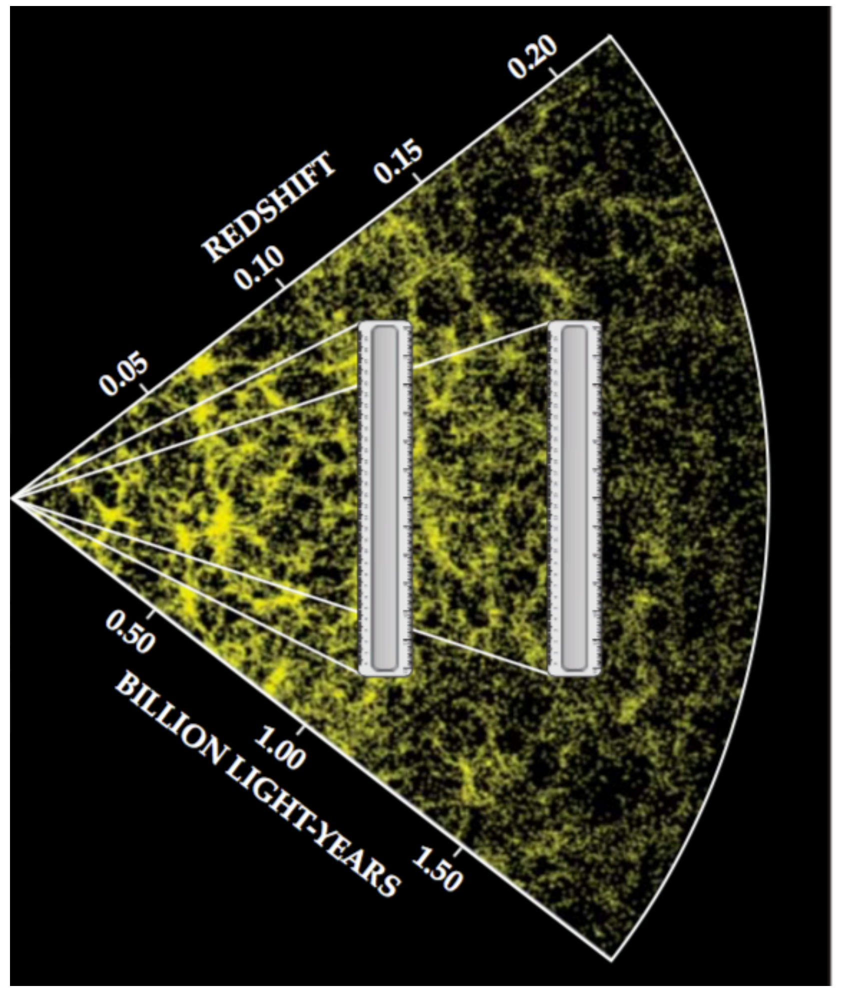

Fiducial DES Y3 BAO analysis

- 7 million red galaxies z= 0.6 to 1.1, 5 tomographic bins
- 10 σ depth of 22, 22, 22.3, and 21 for griz

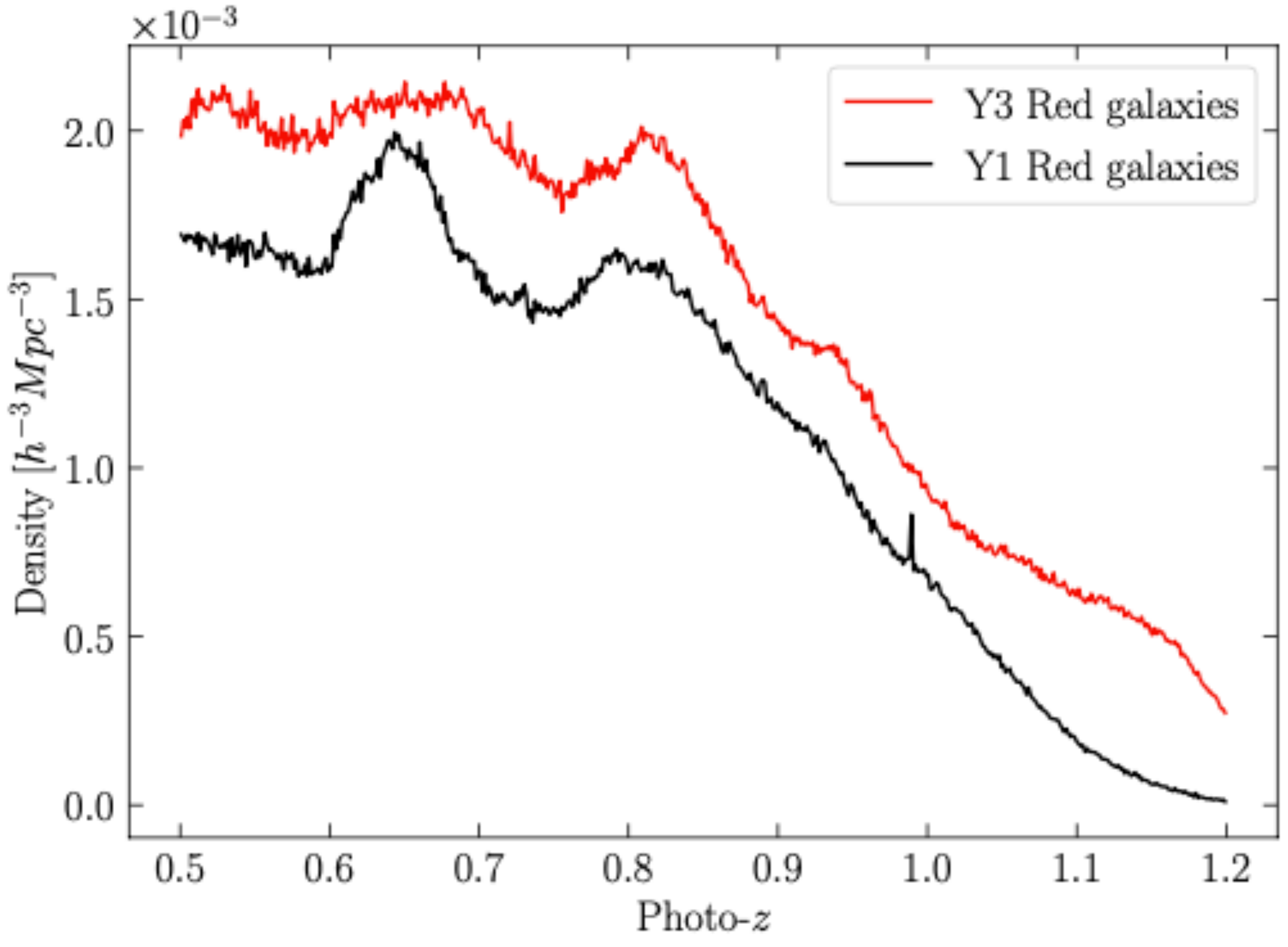

Redshift limits	$\bar{z}$	W_{68}	σ_{68}	Number of galaxies	blind galaxy bias
0.6 < z < 0.7	0.648 ± 0.003	0.0455 ± 0.003	0.021 ± 0.001	1,478,178	1.79 ± 0.09
0.7 < z < 0.8	0.742 ± 0.003	0.0522 ± 0.002	0.025 ± 0.002	1,632,805	1.83 ± 0.10
0.8 < z < 0.9	0.843 ± 0.003	0.0629 ± 0.003	0.029 ± 0.002	1,727,646	2.02 ± 0.12
0.9 < z < 1.0	0.932 ± 0.004	0.0633 ± 0.003	0.030 ± 0.003	1,315,604	2.09 ± 0.14
1.0 < z < 1.1	1.020 ± 0.006	0.0808 ± 0.006	0.040 ± 0.005	877,760	2.4 ± 0.08

Carnero Rosell +, 2107.05477

σ_{68} is the width of the distribution $|z_{\rm photo} - z_{\rm spec}|/(1 + z_{\rm spec})$ and W_{68} is the width of the $z_{\rm spec}$ in the photo-z bin.

Angular clustering statistics

- The BAO is measured using angular correlation function w and angular power spectrum C_ℓ

$$w(\theta, z_{\rm p}, z'_{\rm p}) = \sum_\ell i^\ell \int dz \phi(z|z_{\rm p}) \int dz' \phi(z'|z'_{\rm p}) \mathcal{L}_\ell(\hat{\boldsymbol{s}} \cdot \hat{\boldsymbol{e}}) \int \frac{dk k^2}{2\pi^2} j_\ell(ks) P_\ell(k, z, z')$$

$$P(k, \mu) = (b + \mu^2 f)^2 \left[(P_{\rm lin} - P_{\rm nw}) e^{-k^2 \Sigma_{\rm tot}^2} + P_{\rm nw} \right]$$

$$C_\ell = 2\pi \int_{-1}^{1} d(\cos\theta)\, w(\theta) \mathcal{L}_\ell(\cos\theta)$$

- BAO position in w or C_ℓ is extracted by fitting the full template to the data

$$M(x) = B T_{{\rm BAO},\alpha}(x') + A(x),$$

For w, $x = \theta$, $x' = \alpha\theta$, $T = w$, $A(\theta) = \sum_i \frac{a_i}{\theta^i}$ For C_ℓ, $x = \ell$, $x' = \frac{\ell}{\alpha}$, $T = C_\ell$, $A(\ell) = \sum_i a_i \ell^i$.

Angular BAO measurement

- w and C_ℓ results are consistent with each other

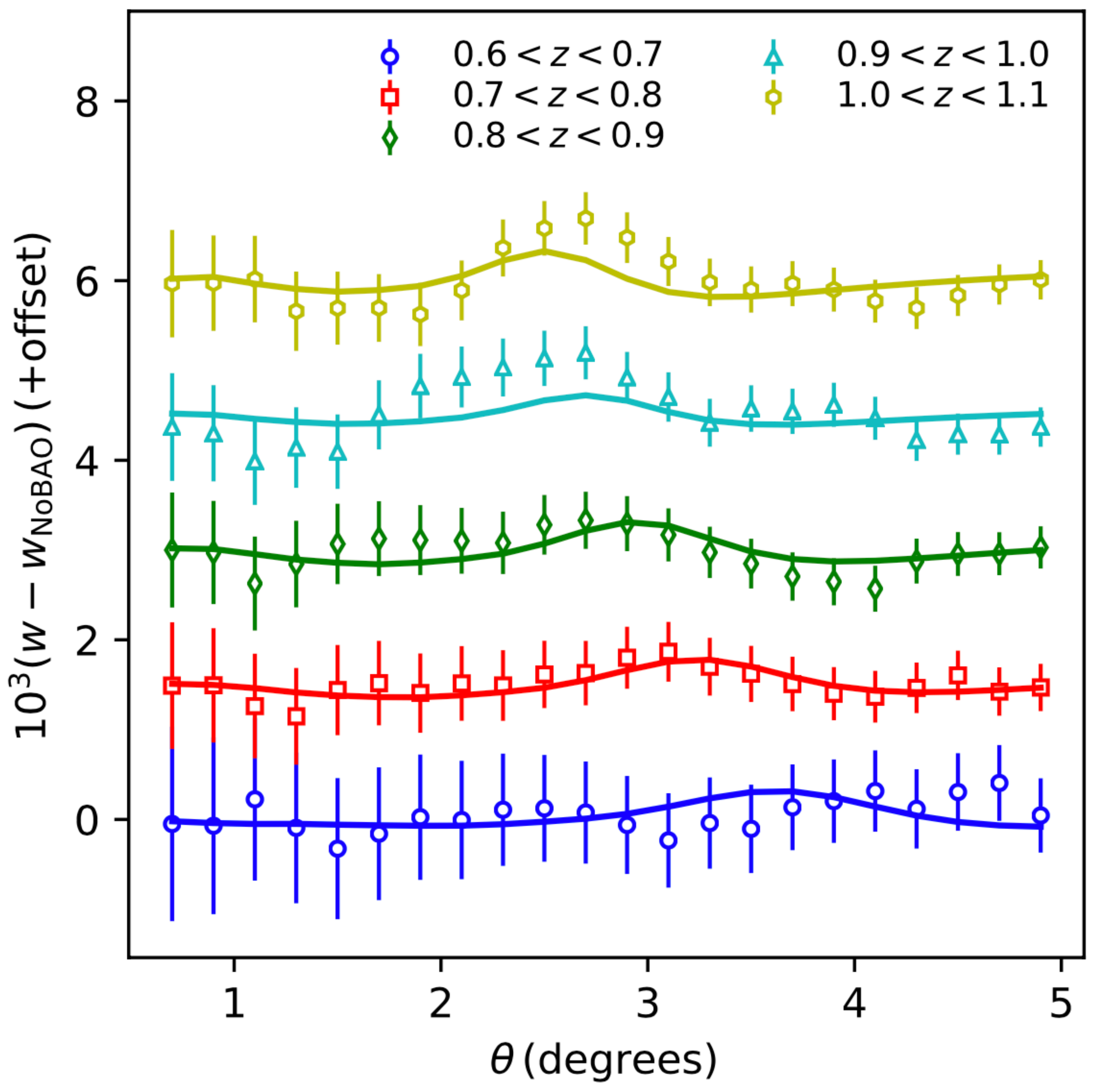

w

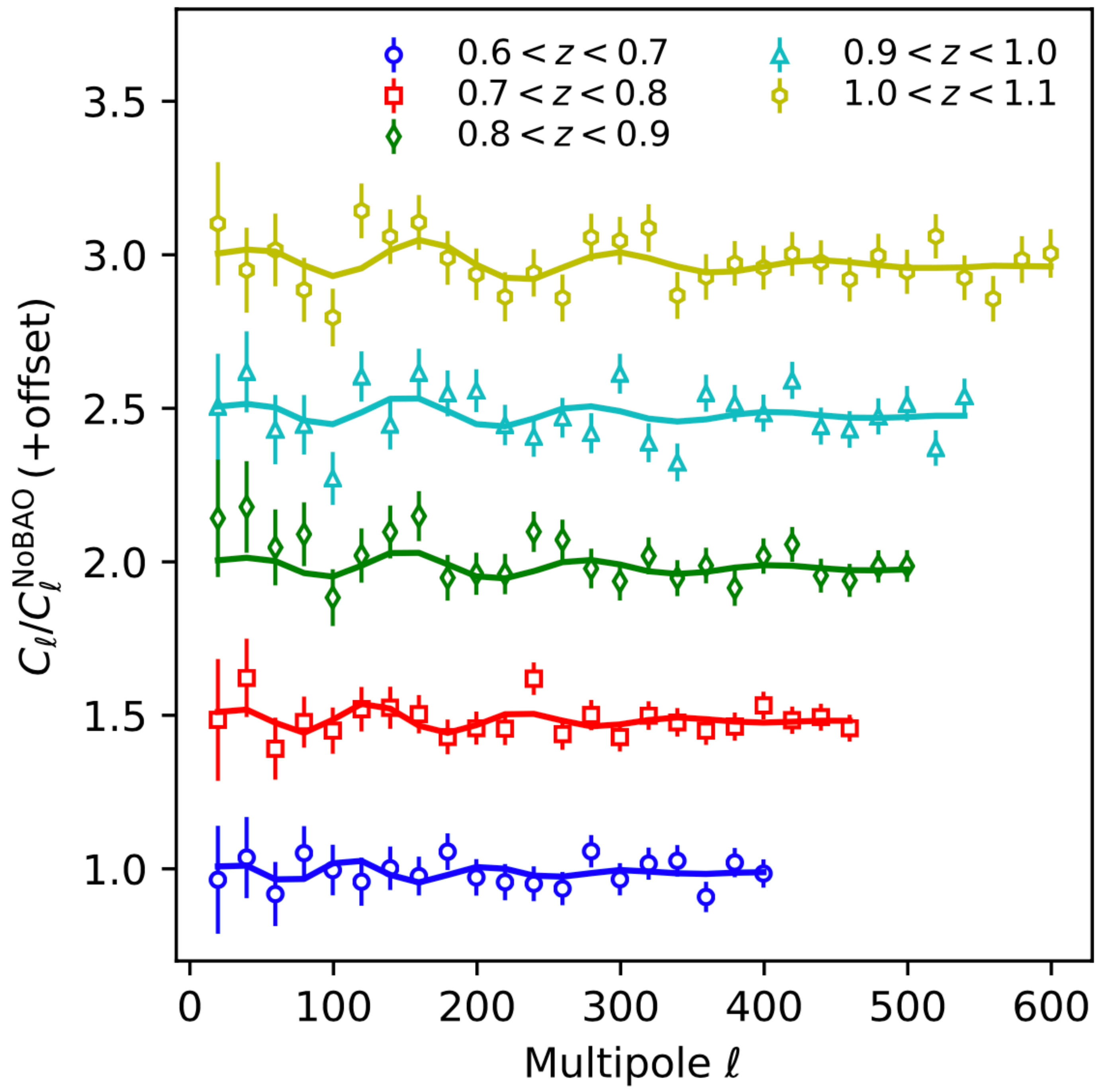

C_ℓ

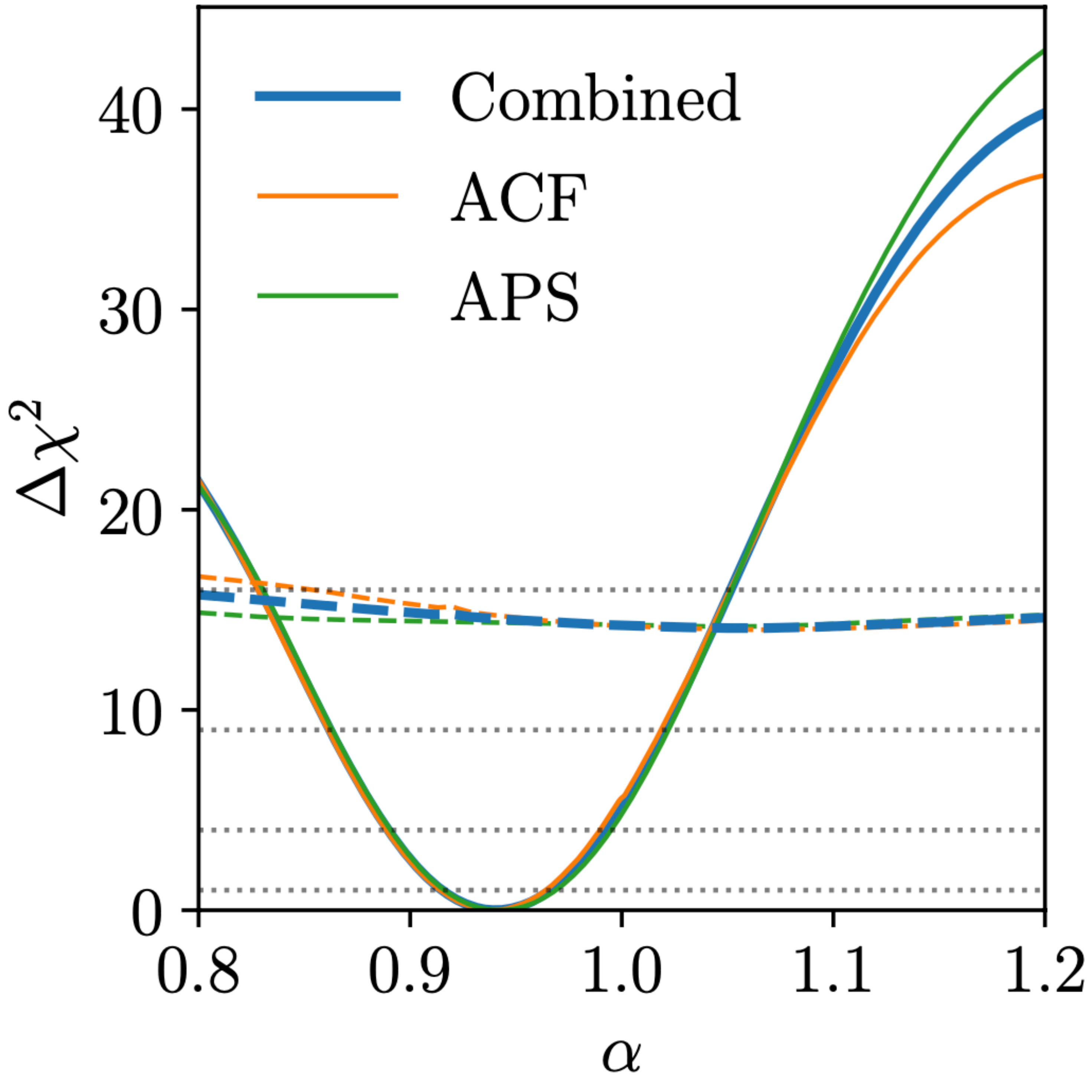

$$\alpha = \frac{\left.\frac{D_{\rm M}}{r_{\rm d}}\right|_{\rm data}}{\left.\frac{D_{\rm M}}{r_{\rm d}}\right|_{\rm fid}}$$

DES collaboration, 2107.05477

About 2 sigma deviation from the Planck results

DES Y3 BAO constraints

- $D_\mathrm{M}/r_\mathrm{d} = 18.92 \pm 0.51$, 2.5% measurement of the BAO at z= 0.83
- Most precise BAO measurement from photometric surveys
- $D_\mathrm{M}/r_\mathrm{d}$ is at 2.3σ deviation from the Planck results, need more data and alternative analyses to corroborate

$$\alpha = \frac{\frac{D_\mathrm{M}}{r_\mathrm{d}}\Big|_\mathrm{data}}{\frac{D_\mathrm{M}}{r_\mathrm{d}}\Big|_\mathrm{fid}}$$

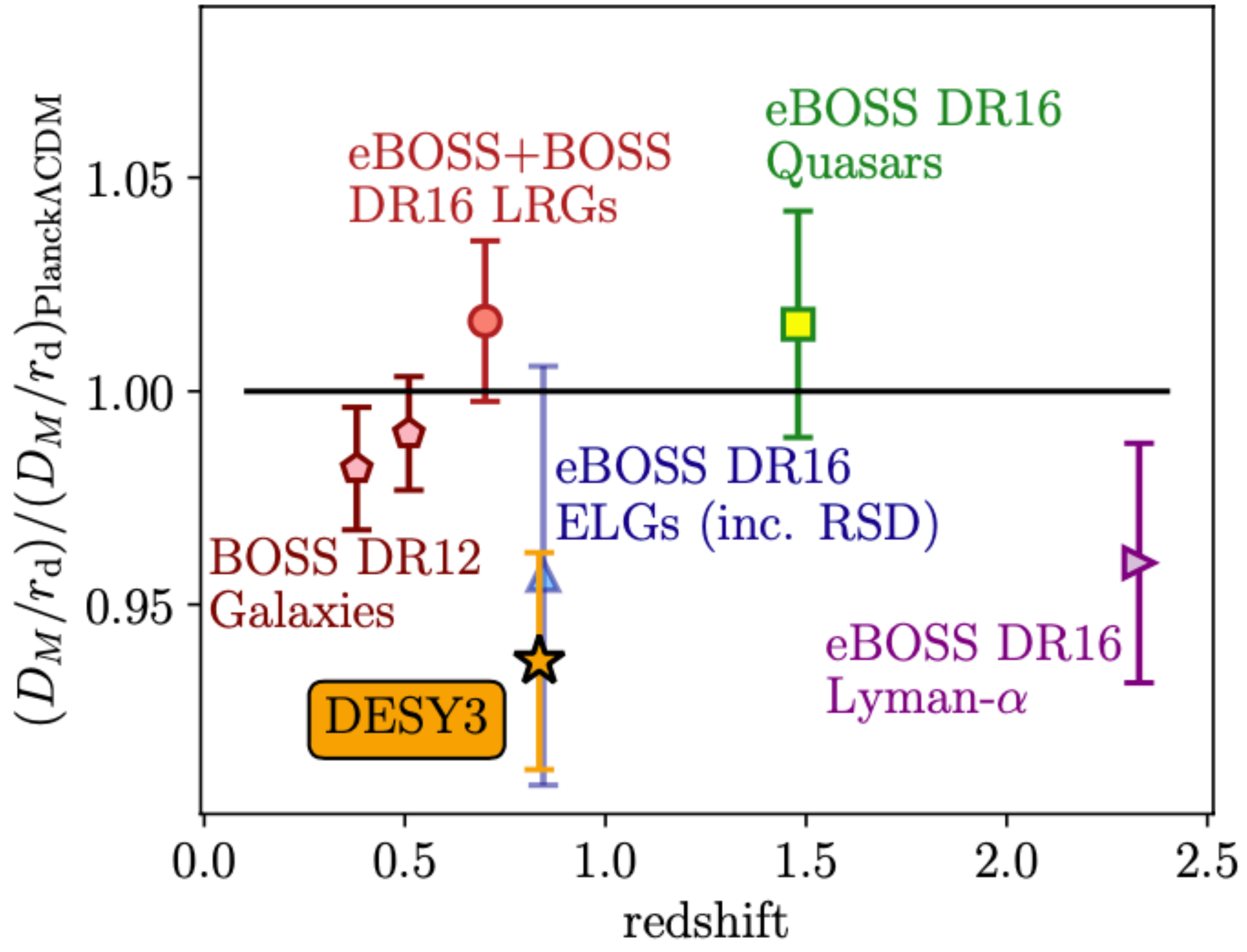

DES collaboration, 2107.05477

Three-dimensional correlation analysis

- Compute the 3D correlation function ξ akin to 3D analysis

Ross +, 1705.05442

- Compress info in the whole redshift range into a single data vector. Include some radial info
- Need to take care of the evolving dn/dz
- Radial direction is smeared, need projection

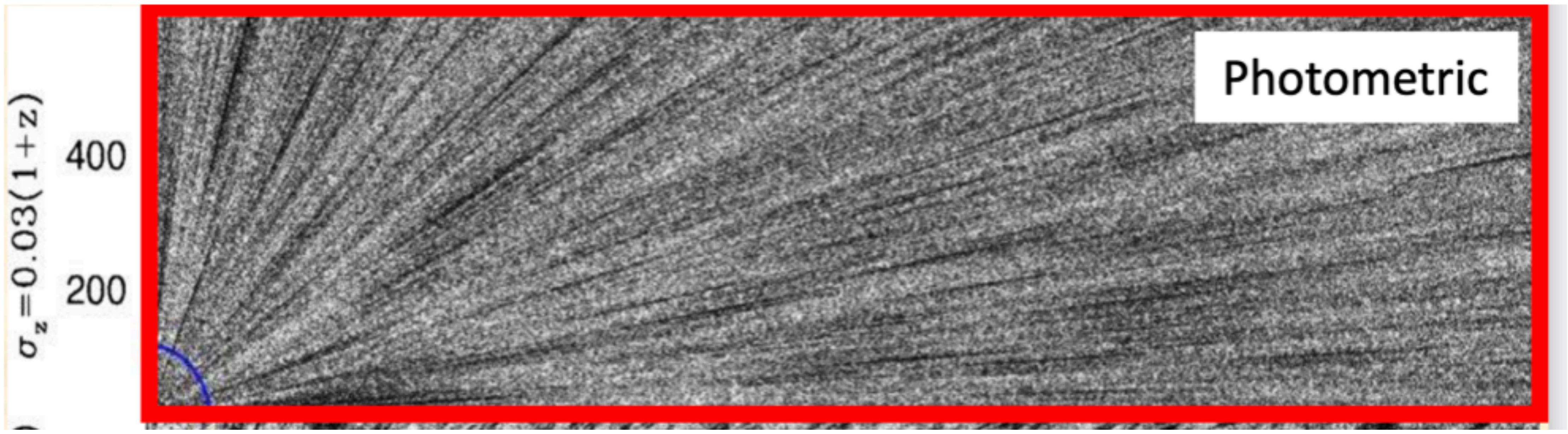

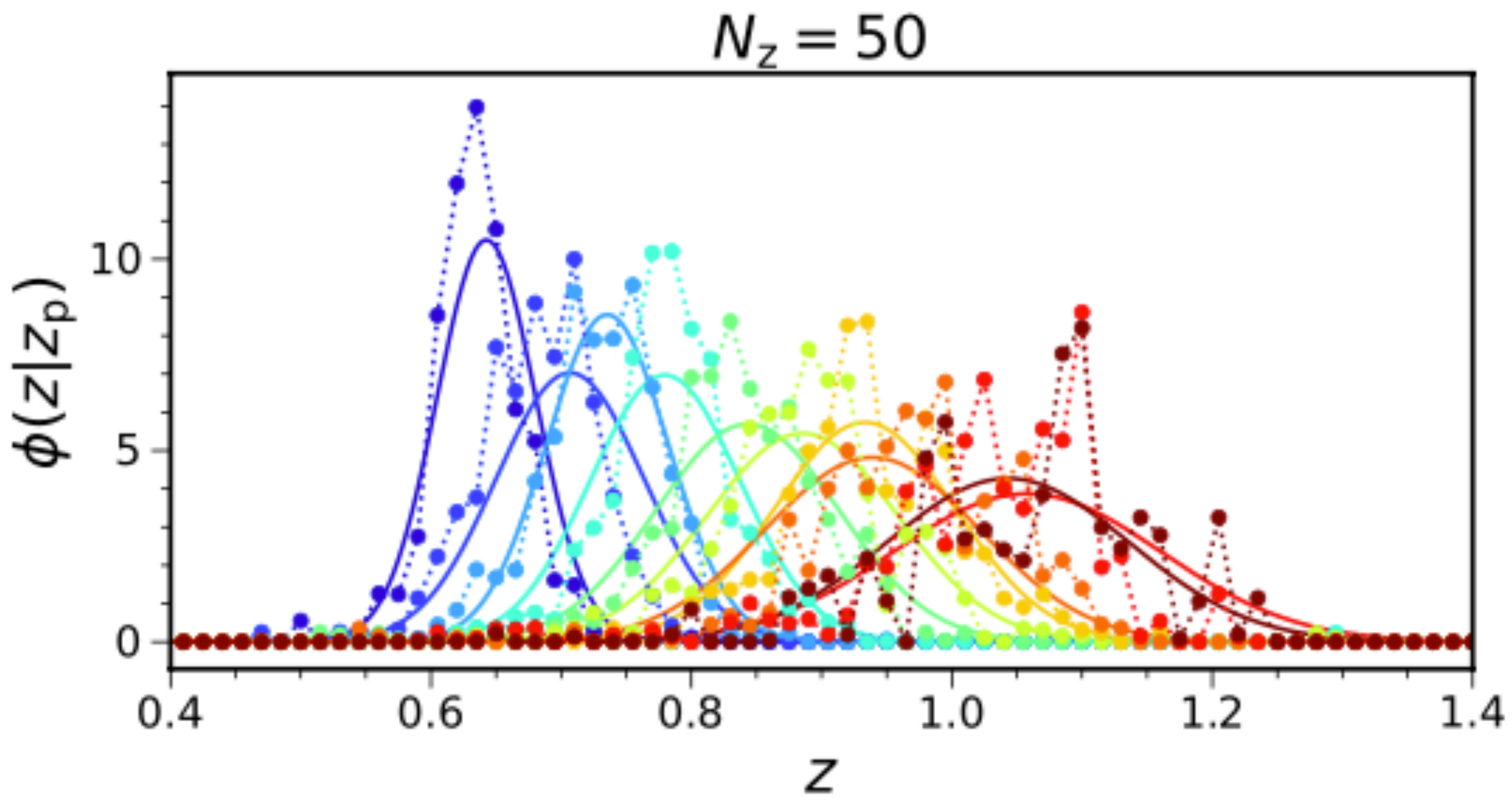

3D correlation analysis for photometric data

- For $\sigma_z \geq 0.02$, only effectively probes the transverse information, the transverse BAO is preserved

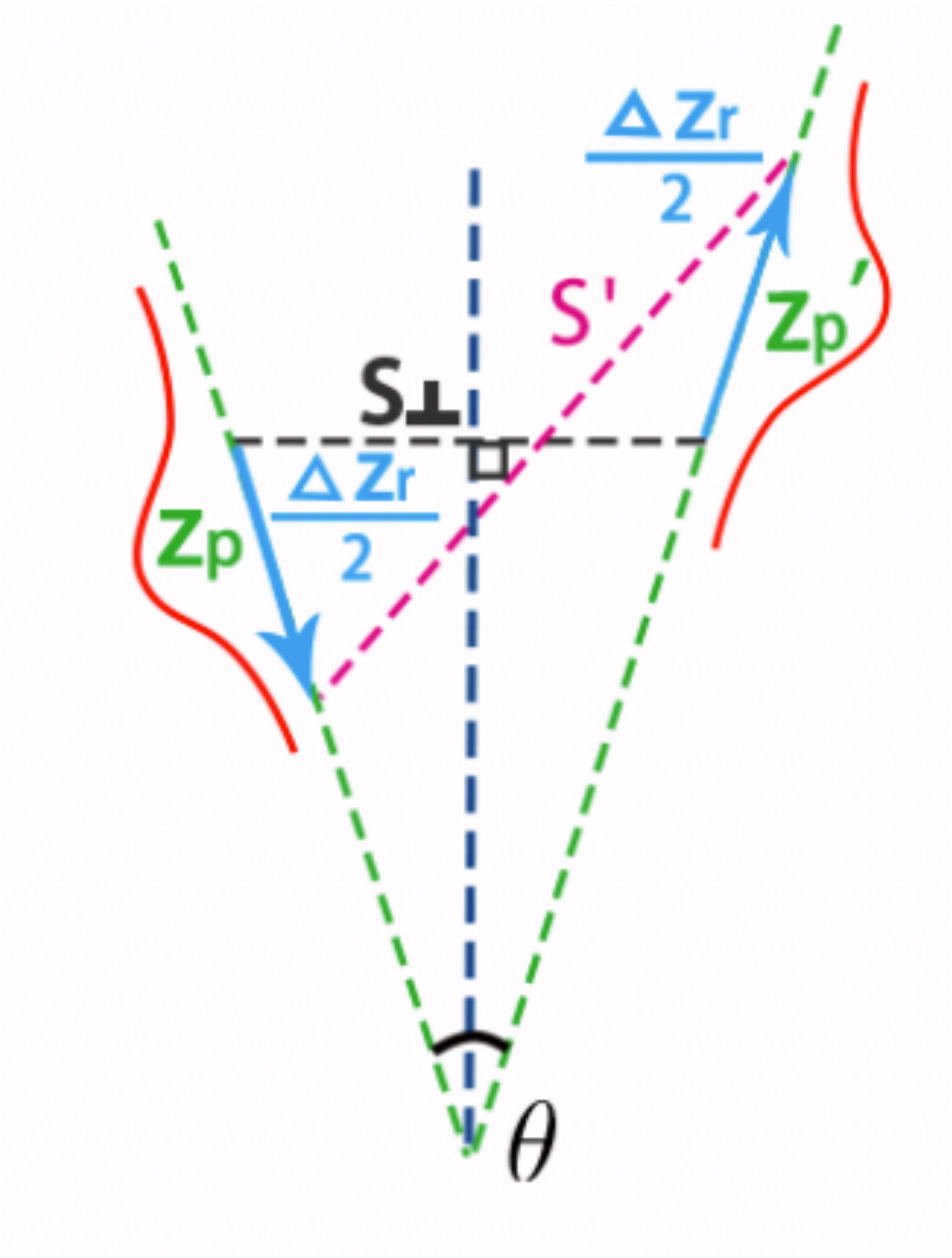

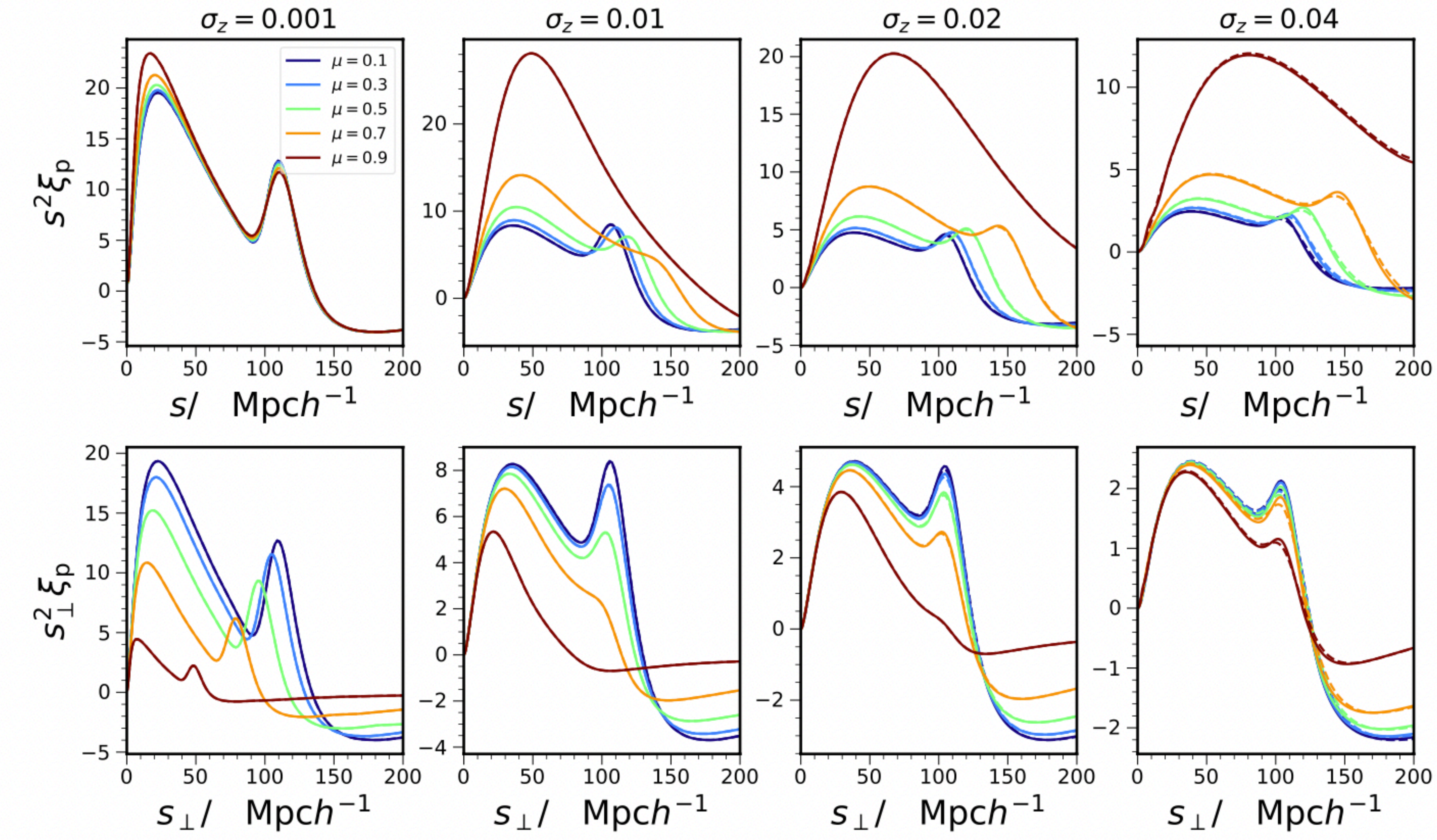

Ross +, 1705.05442 KCC +, 2110.13332

$\xi_{\rm p}$ template

- Obtained by mapping the general w template to $\xi_{\rm p}$

$$w_{ij}(\theta) = \sum_{\ell=0,2,4} i^\ell \int dz \phi(z|z_{\rm p}) \int dz' \phi(z'|z'_{\rm p}) \times \mathcal{L}_\ell(\hat{\mathbf{s}} \cdot \hat{\mathbf{e}}) \int \frac{dk k^2}{2\pi^2} j_\ell(ks) P_\ell(k, z, z'),$$

- Loop over ijk that satisfy the bin conditions, ensure the evolving dn/dz window is accounted for

$$\xi_{\rm p}(s, \mu) = \frac{\sum_{ijk} f_{ijk} w_{ij}(\theta_k)}{\sum_{ijk} f_{ijk}}$$

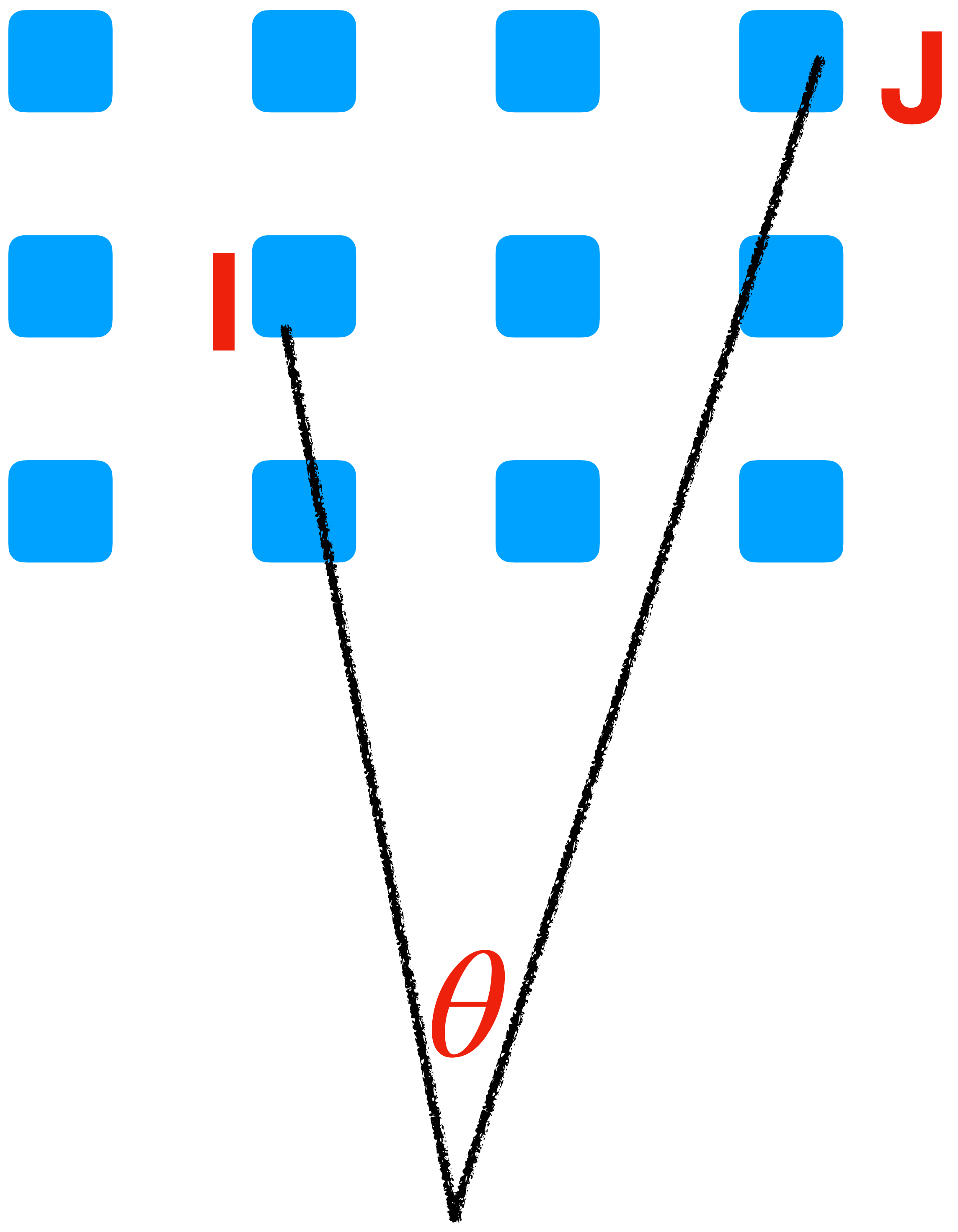

KCC +, 2110.13332

$\xi_{\rm p}$ template

- Photo-z uncertainties, the radial info, especially the radial BAO is erased
- Project $\xi_{\rm p}(s, \mu)$ to the transverse direction

KCC +, 2110.13332

$$\xi_{\rm p}(s_\perp) = \frac{\sum_i \xi_{\rm p}(s, \mu_i) W(\mu_i)}{\sum_i W(\mu_i)}$$

Tophat: equal weighting, sub-optimal

Gaussian: suppress the pairs with low signal to noise

Theory vs mock measurement

- ICE-COLA mocks, data include realistic photo-z uncertainties
- The theory template is in good agreement with the mock measurement

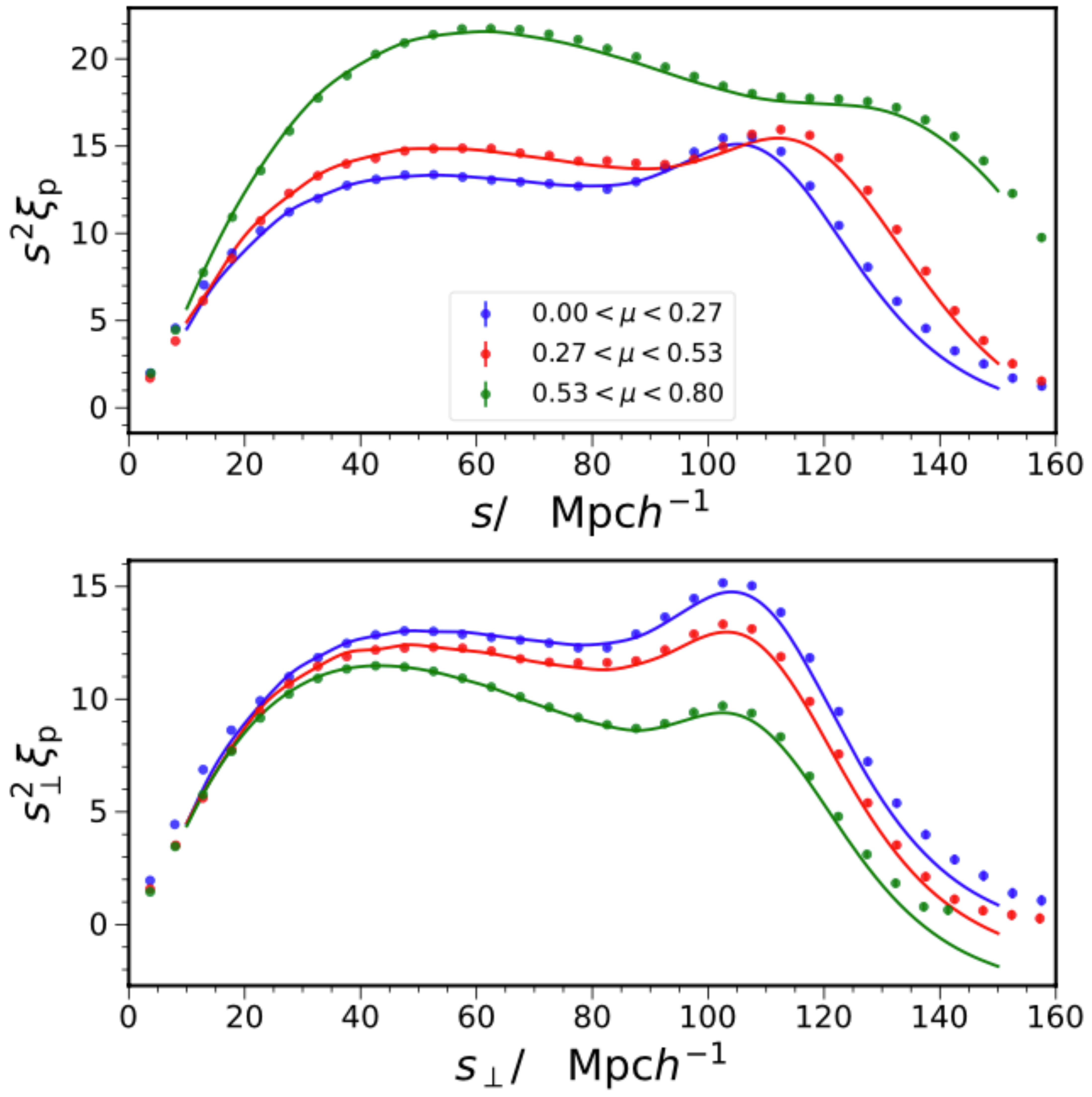

Testing the stacking window on mocks

- Gaussian window behaves more stably as the width of the window decreases b/c it gives more weight to the pairs with high S/N

Top-hat

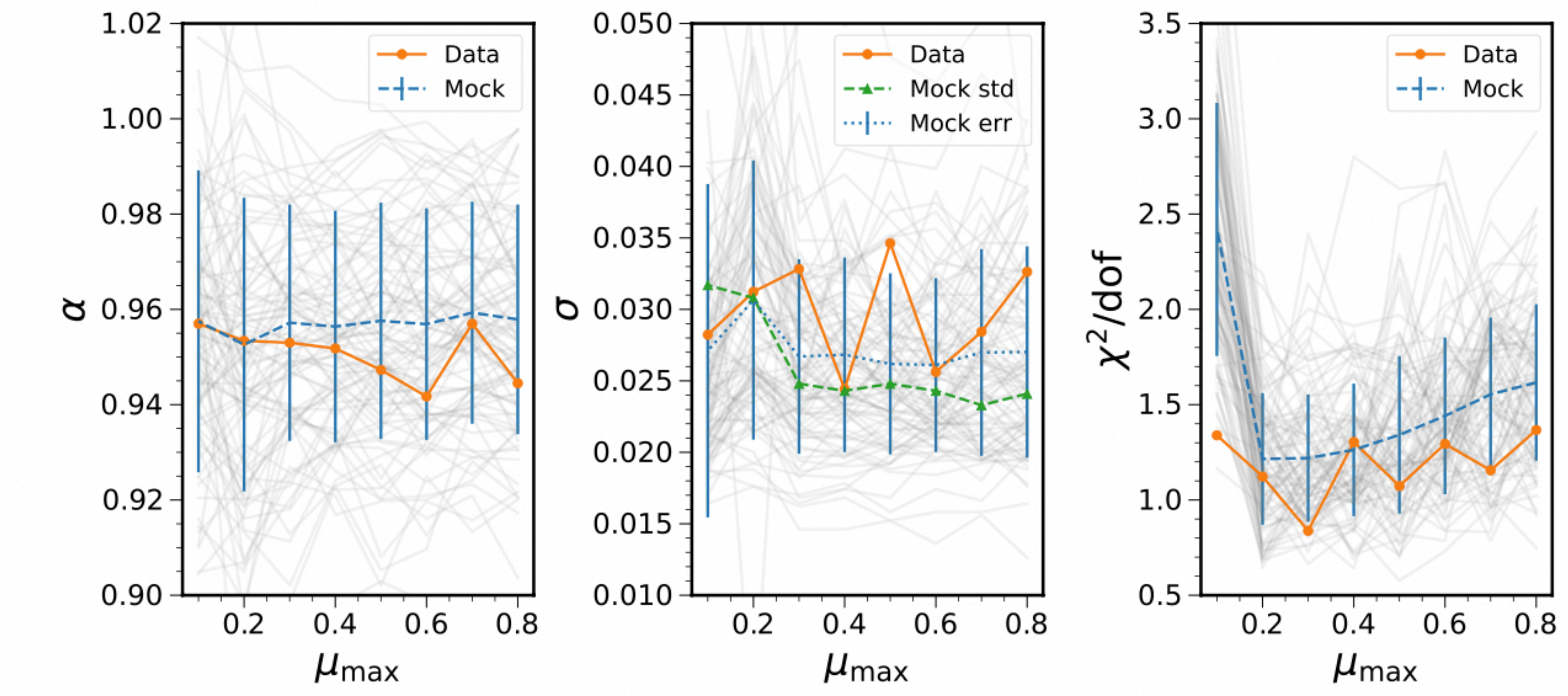

Gaussian

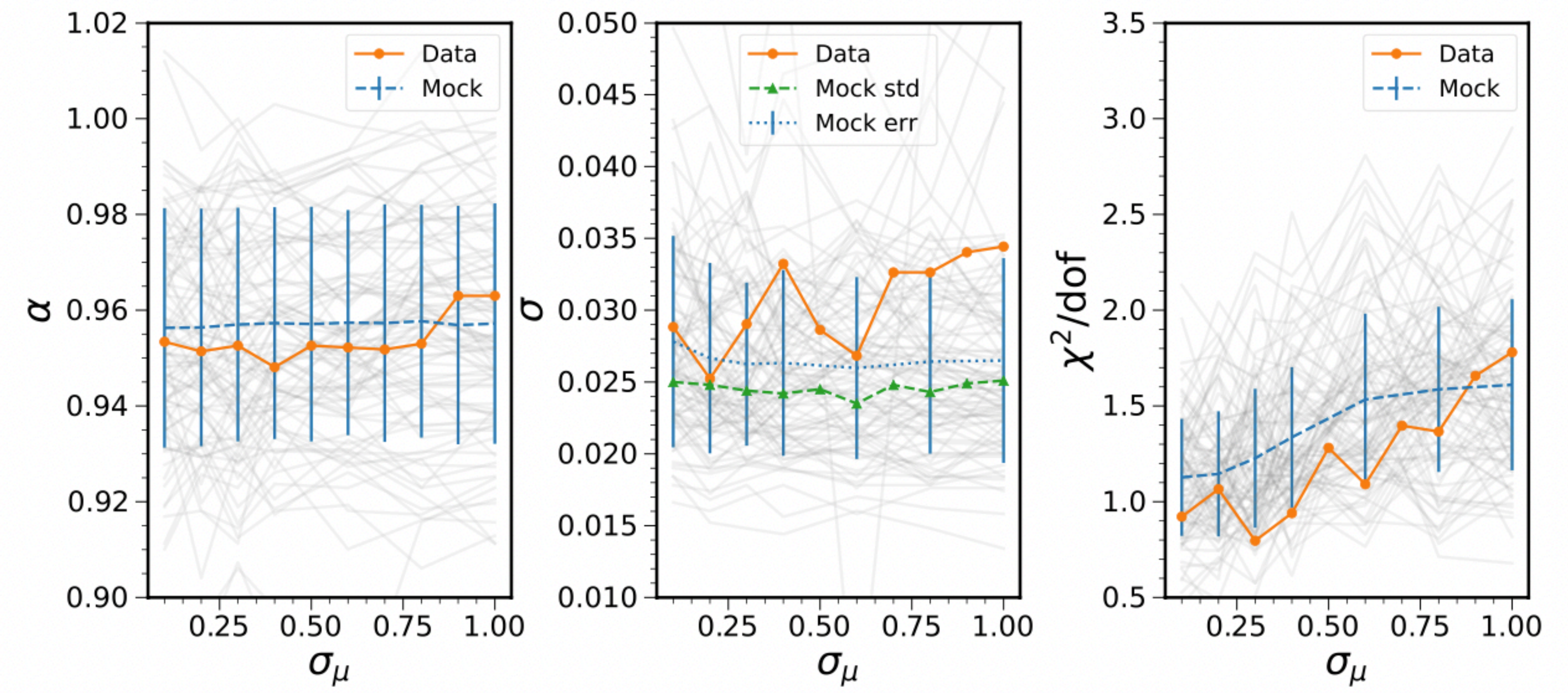

More stable mean and error bar estimates, more consistent χ^2/dof, Gaussian window is preferred

ξ_{p} covariance

- Mapping the general w covariance to ξ_{p} one

$$\mathrm{Cov}[\xi_{\mathrm{p}}(s_\perp), \xi_{\mathrm{p}}(s'_\perp)]$$
$$= \frac{\sum_i \sum_j W(\mu_i) W(\mu_j) \mathrm{Cov}(\xi_{\mathrm{p}}(s, \mu_i), \xi_{\mathrm{p}}(s', \mu_j))}{\sum_i W(\mu_i) \sum_j W(\mu_j)}$$

$$\mathrm{Cov}[\hat{w}_{ij}(\theta), \hat{w}_{mn}(\theta')] = \sum_\ell \frac{(2\ell+1)}{(4\pi)^2 f_{\mathrm{sky}}} \bar{\mathcal{L}}_\ell(\cos\theta) \bar{\mathcal{L}}_\ell(\cos\theta')$$
$$\left[\left(C_\ell^{im} + \frac{\delta_{\mathrm{K}}^{im}}{\bar{n}_i}\right)\left(C_\ell^{jn} + \frac{\delta_{\mathrm{K}}^{jn}}{\bar{n}_j}\right) + \left(C_\ell^{in} + \frac{\delta_{\mathrm{K}}^{in}}{\bar{n}_i}\right)\left(C_\ell^{jm} + \frac{\delta_{\mathrm{K}}^{jm}}{\bar{n}_j}\right)\right]$$

Finite bin width correction
Mask correction

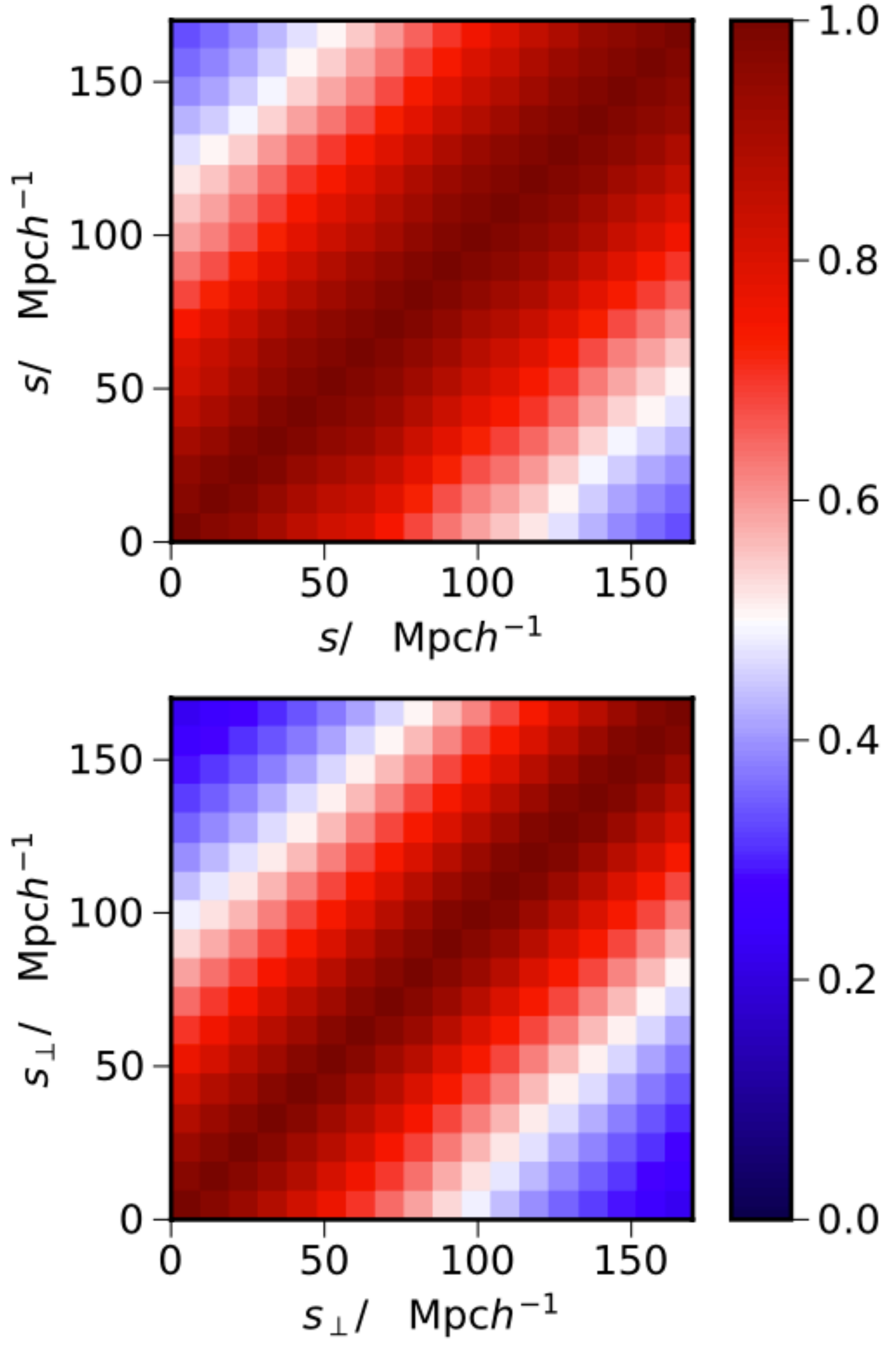

Correlation btw ξ_p and angular statistics

- The correlation btw ξ_p and angular statistics (w or C_ℓ) is low, serves as a more independent statistic

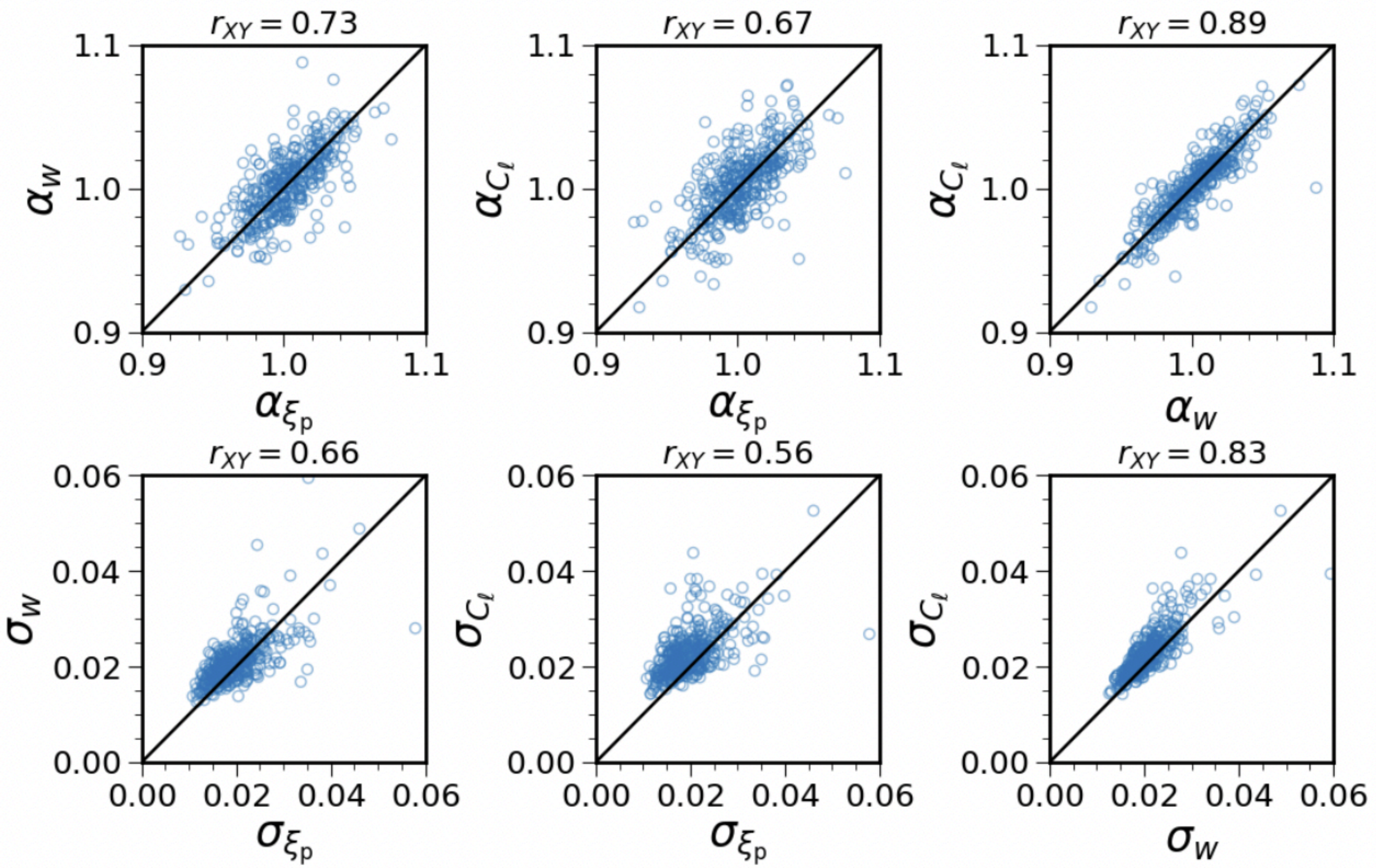

BAO sample

- BAO sample, 7.03 million red galaxies in the redshift range of [0.6,1.1] over a footprint of 4108 deg^2

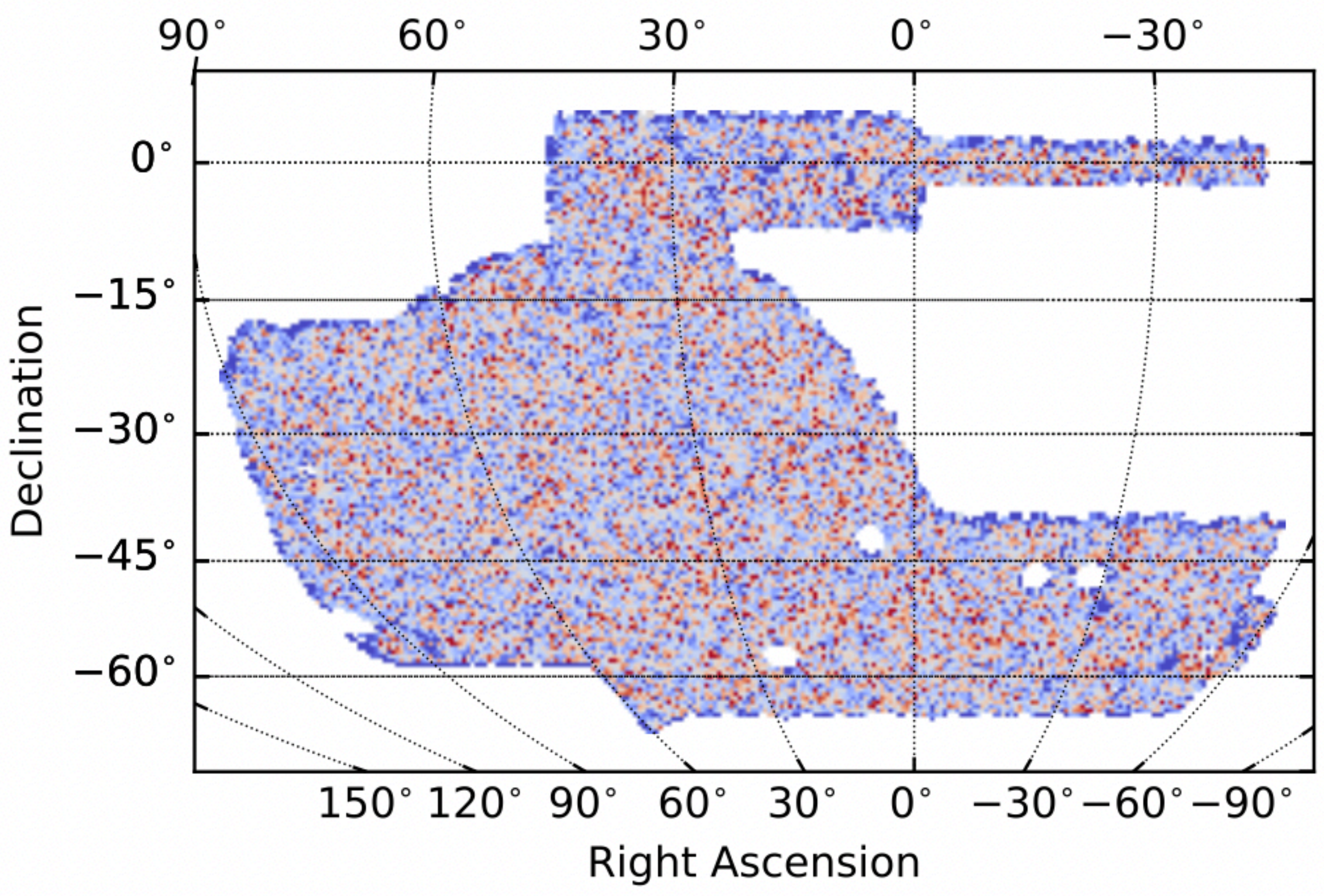

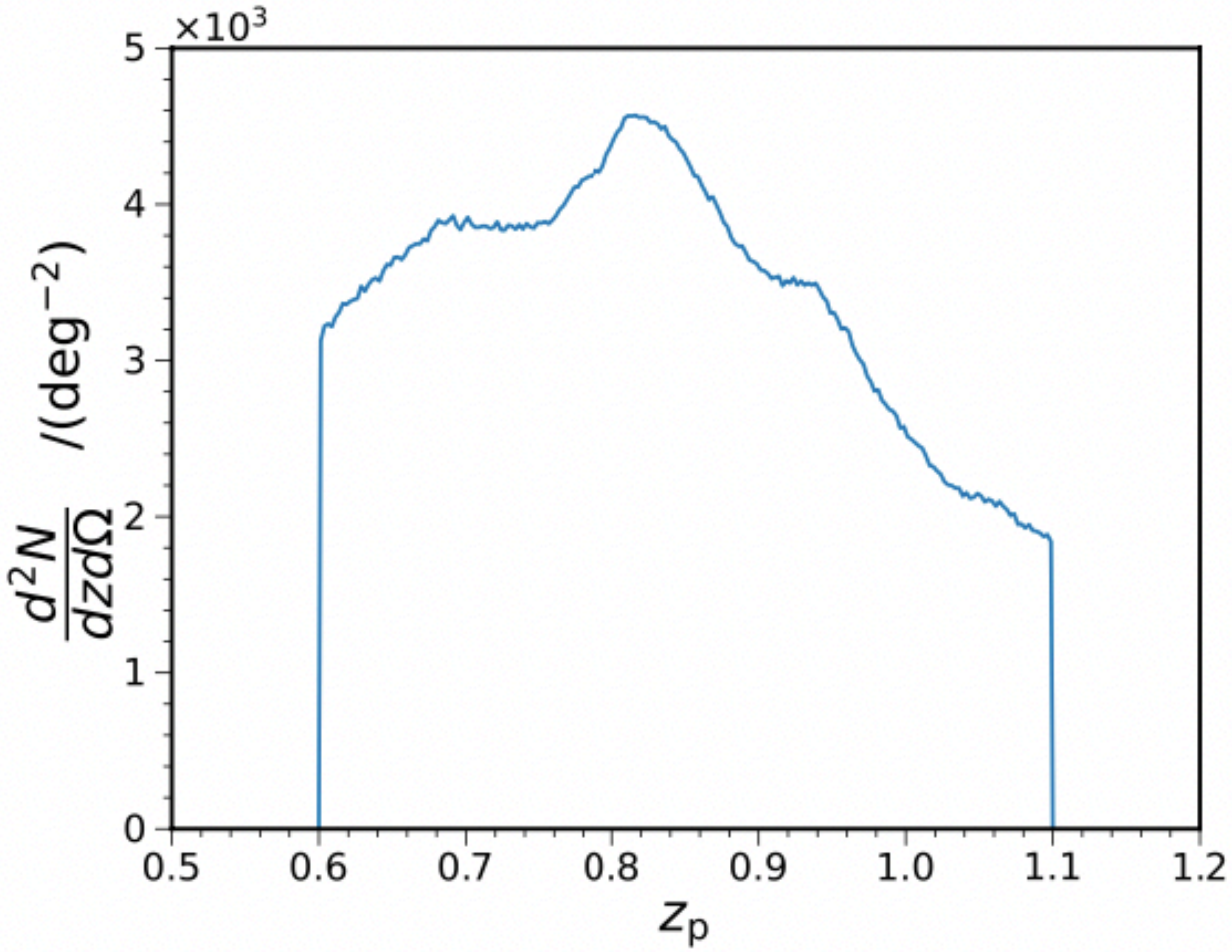

True-z distribution

- Photo-z derived from DNF, true redshift distribution estimated with the VIPERS spec-z sample

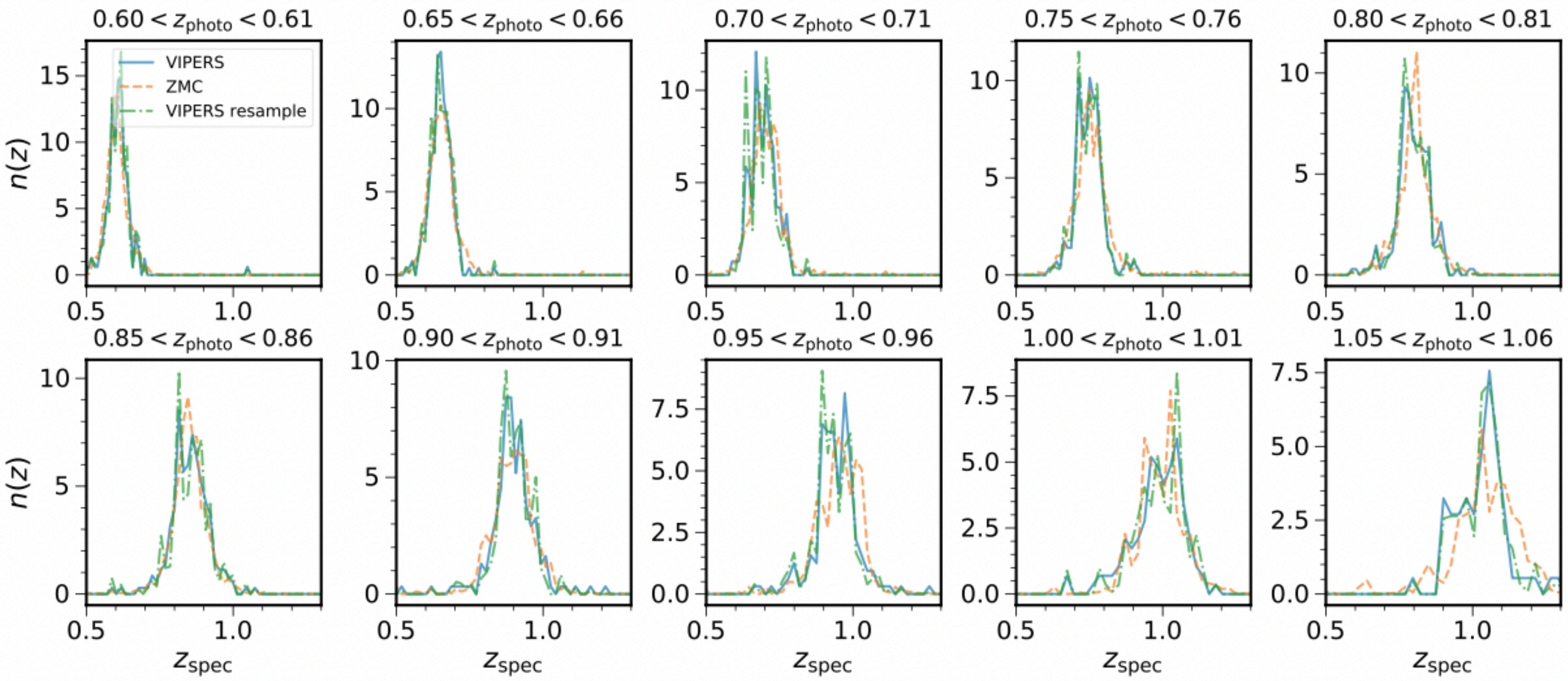

BAO measurements

- $\xi_{\rm p}$ constraint on α: 0.953 ± 0.029 (Gaussian) and 0.945 ± 0.033 (Top-hat)
- Consistent with w: 0.937 ± 0.025
- Deviation from Planck is reduced to 1.6 σ

Planck fiducial cosmology, $\alpha = 1$

$$\alpha = \frac{\frac{D_{\rm M}}{r_{\rm d}}\Big|_{\rm data}}{\frac{D_{\rm M}}{r_{\rm d}}\Big|_{\rm fid}}$$

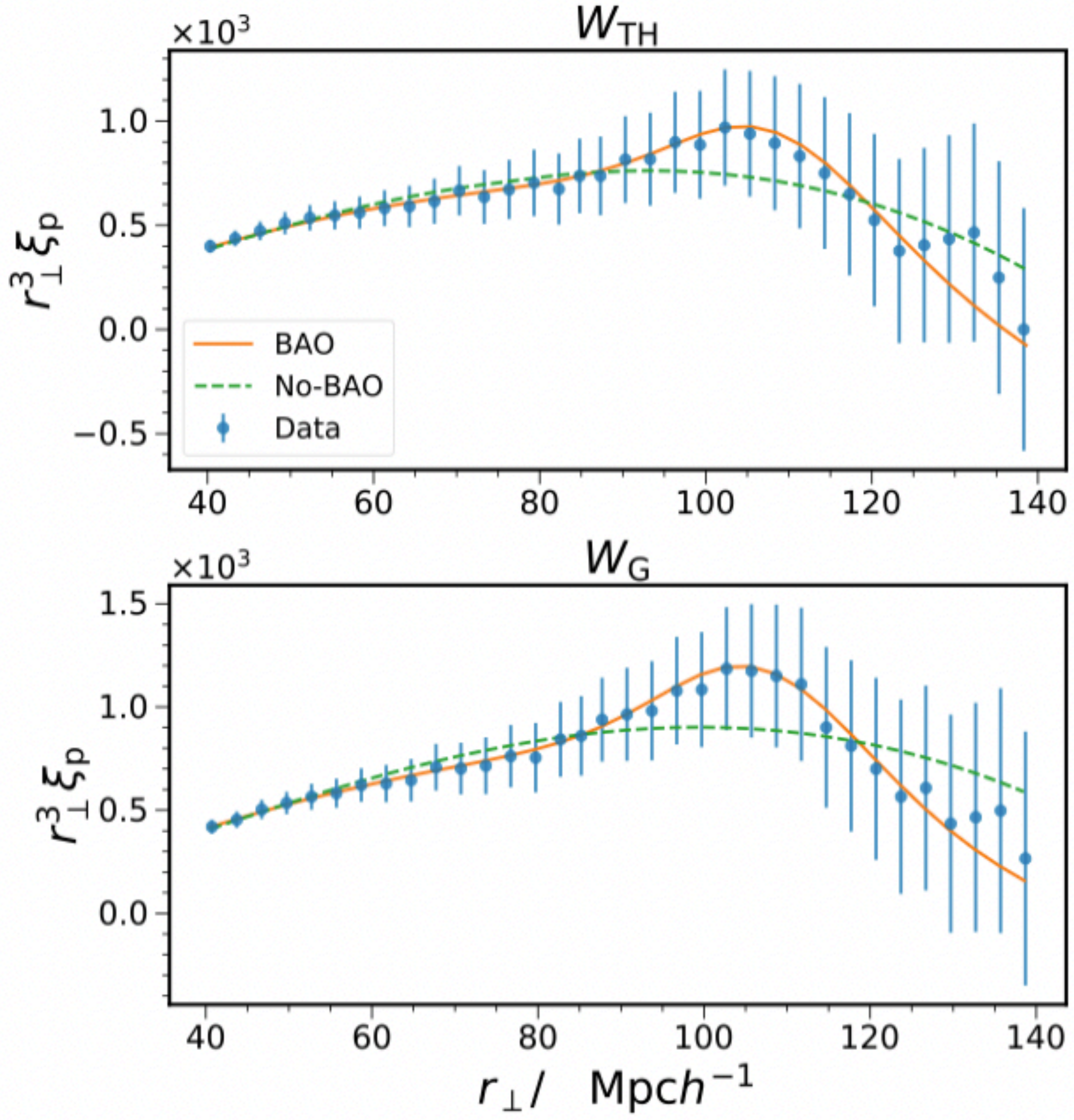

Individual bin fit results

- Individual tomographic bins, ξ_{p} gives comparable or even tighter constraint than w
- The BAO signals are heterogeneous across redshift, deviation from Planck mainly driven by the last bin

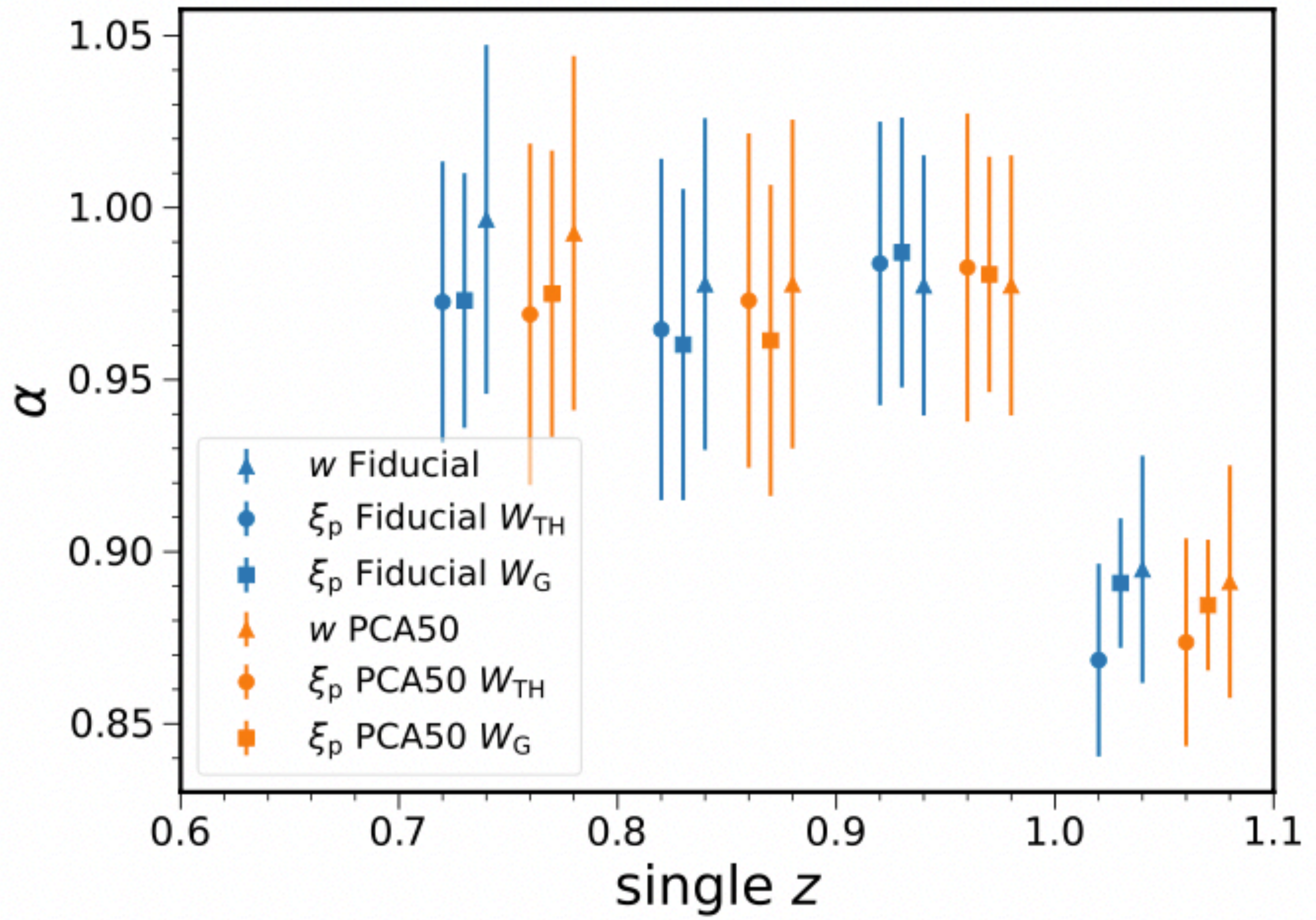

Error bars in heterogeneous mocks

- In heterogeneous mocks, the probability of getting $\xi_{\rm p}$ with error bar larger than w is enhanced

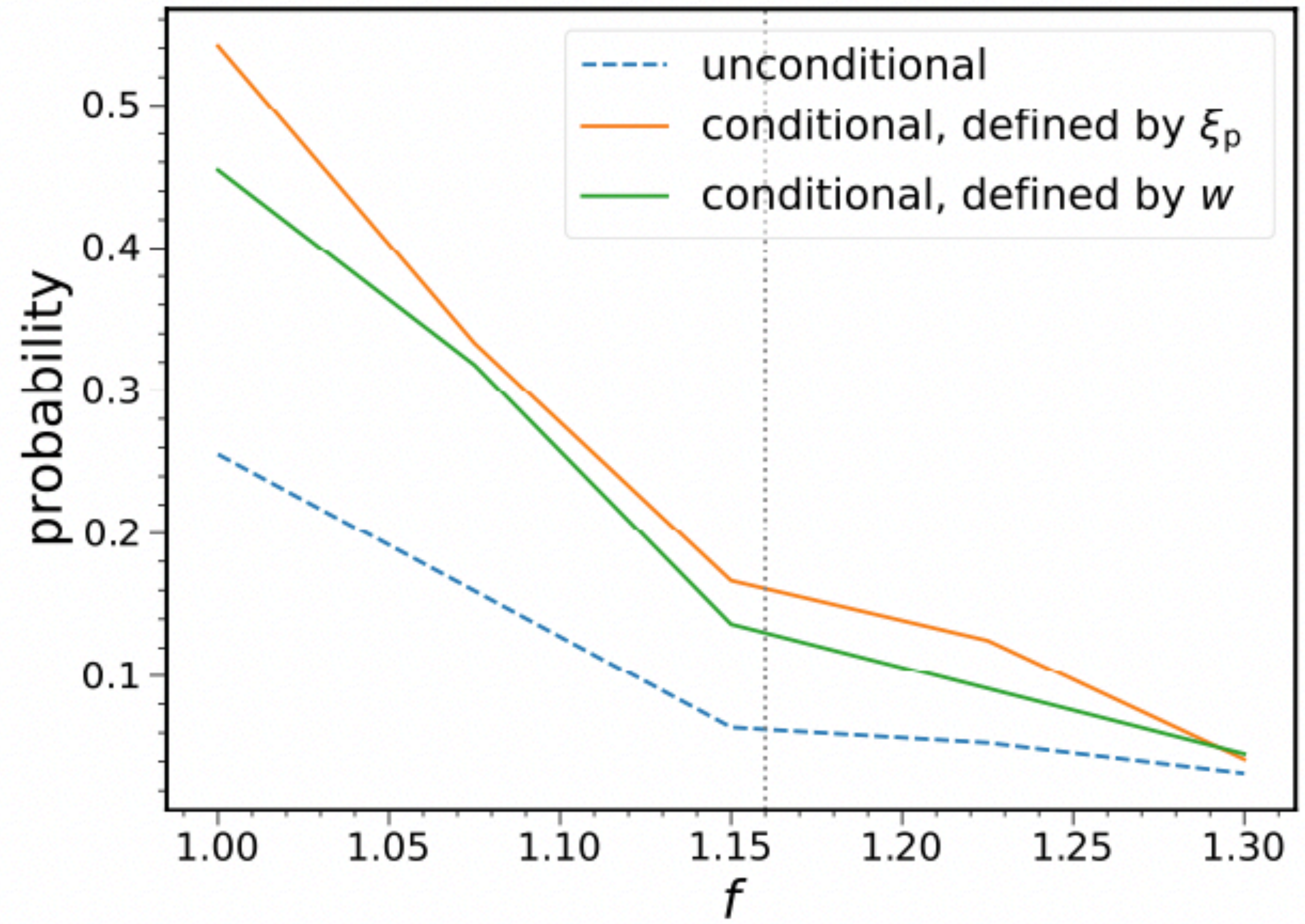

Measurements in homogeneous sample

- The combo 2-4 bins contains consistent BAO signals, the resultant constraint from 0.977 ± 0.026 (Gaussian) and 0.975 ± 0.033 (Top-hat) vs 0.978 ± 0.027 (w)
- $\xi_{\rm p}$ combines the signals at the level of data vector, while w effectively combines likelihood
- Caveat: combining likelihood always shrinks the error bar

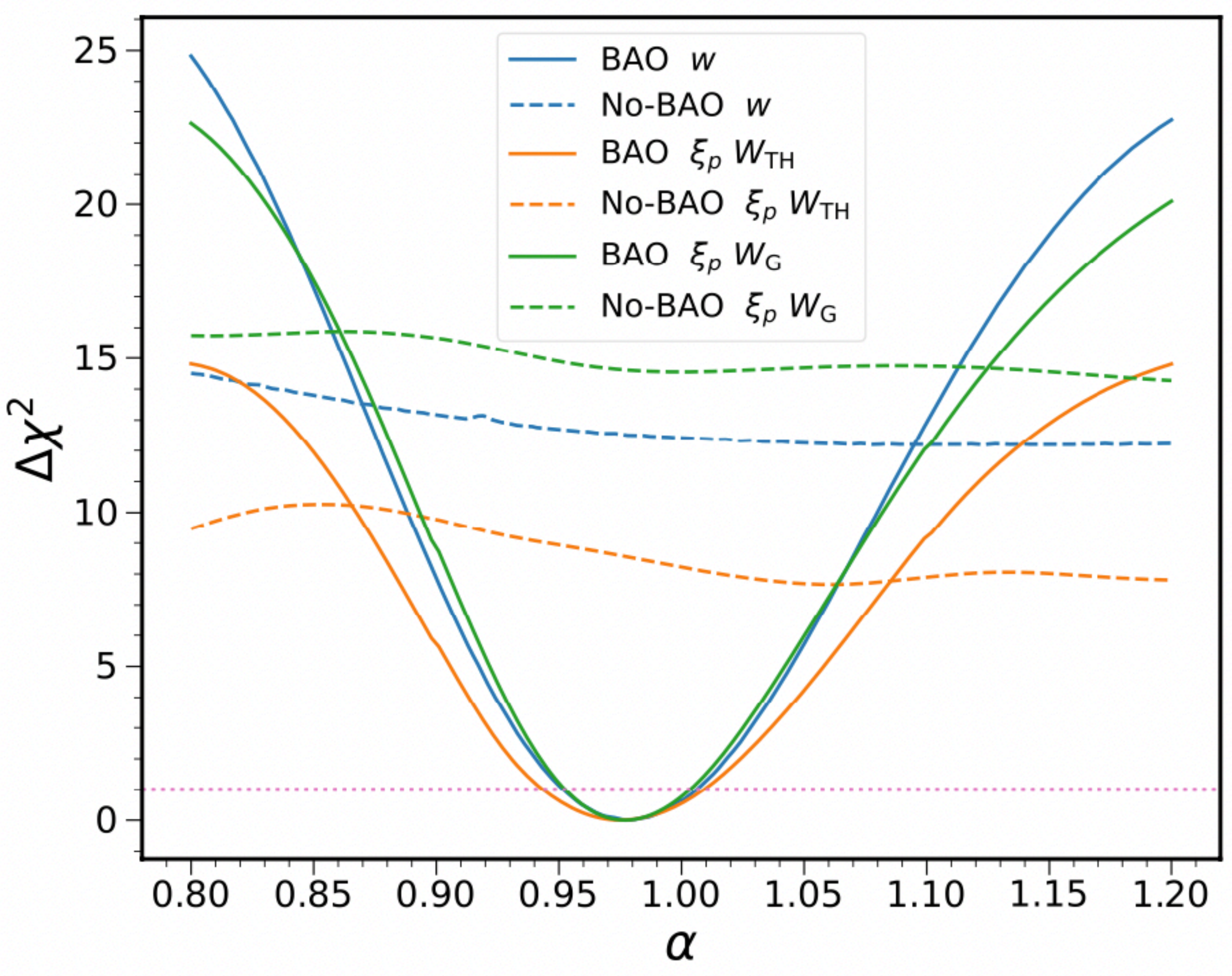

Robustness tests

- ξ_p is generally more sensitive to photo-z noise than w b/c (1) it measures correlation after projection (2) it combines signals at the level of data vector
- Gaussian window is more stable than top-hat as it puts more weight to the transverse pairs

Case	ξ_p: W_G	ξ_p: W_TH	w
Default	0.953 ± 0.029 (21.5/29)	0.945 ± 0.033 (33.4/29)	0.937 ± 0.025 (95.2/89)
No sys. corr.	0.942 ± 0.029 (39.7/29)	* 0.938 ± 0.033 (46.4/29)	0.935 ± 0.026 (94.6/89)
sys − PCA50	0.945 ± 0.029 (22.8/29)	0.943 ± 0.028 (36.0/29)	0.937 ± 0.025 (94.9/89)
$n(z)$ Z_MC	0.948 ± 0.029 (21.6/29)	* 0.943 ± 0.034 (33.6/29)	0.935 ± 0.025 (95.6/89)
MICE template	0.989 ± 0.038 (53.5/29)	* 0.988 ± 0.032 (78.5/29)	0.980 ± 0.026 (95.1/89)
MICE cov.	0.956 ± 0.021 (23.7/29)	* 0.955 ± 0.025 (41.0/29)	0.936 ± 0.021 (125.8/89)
MICE cosmology	0.996 ± 0.026 (59.3/29)	0.995 ± 0.021 (90.7/29)	0.977 ± 0.022 (125.8/89)
Unmodified cov.	0.956 ± 0.030 (21.3/29)	0.953 ± 0.035 (32.7/29)	—
$[70, 130]\,\mathrm{Mpc}\,h^{-1}$	0.955 ± 0.030 (11.7/16)	0.965 ± 0.031 (17.1/16)	—
$\Delta r = 5\,\mathrm{Mpc}\,h^{-1}$	0.953 ± 0.030 (19.1/15)	0.953 ± 0.036 (16.2/15)	—
$\Delta r = 2\,\mathrm{Mpc}\,h^{-1}$	0.949 ± 0.028 (38.1/44)	0.941 ± 0.031 (44.5/45)	—
No bin 1	0.976 ± 0.024 (29.5/29)	* 0.960 ± 0.030 (38.7/29)	0.948 ± 0.026 (67.8/71)
No bin 2	0.928 ± 0.034 (19.0/29)	* 0.931 ± 0.034 (32.4/29)	0.929 ± 0.026 (80.7/71)
No bin 3	0.938 ± 0.034 (27.0/29)	* 0.941 ± 0.038 (38.7/29)	0.935 ± 0.028 (78.4/71)
No bin 4	0.928 ± 0.033 (24.7/29)	* 0.943 ± 0.034 (38.8/29)	0.925 ± 0.028 (70.0/71)
No bin 5	0.950 ± 0.030 (21.5/29)	* 0.959 ± 0.029 (40.6/29)	0.967 ± 0.026 (82.3/71)

Angular vs Projected 3D

	Angular analysis Projection and then clustering measurement	Projected 3D Clustering measurement and then projection
Pros	**Angle only, cosmology-independent**	**Effective to condense the data Include some radial info**
Cons	**Explicit bin division, loss of radial info**	**Need cosmology for distance computation More sensitive to noise**

Both statistics offer important crosschecks on each other.

Y6 BAO analysis

- Same footprint, but deeper magnitude

- ξ_p, along with angular statistics, is adopted for fiducial Y6 BAO analysis

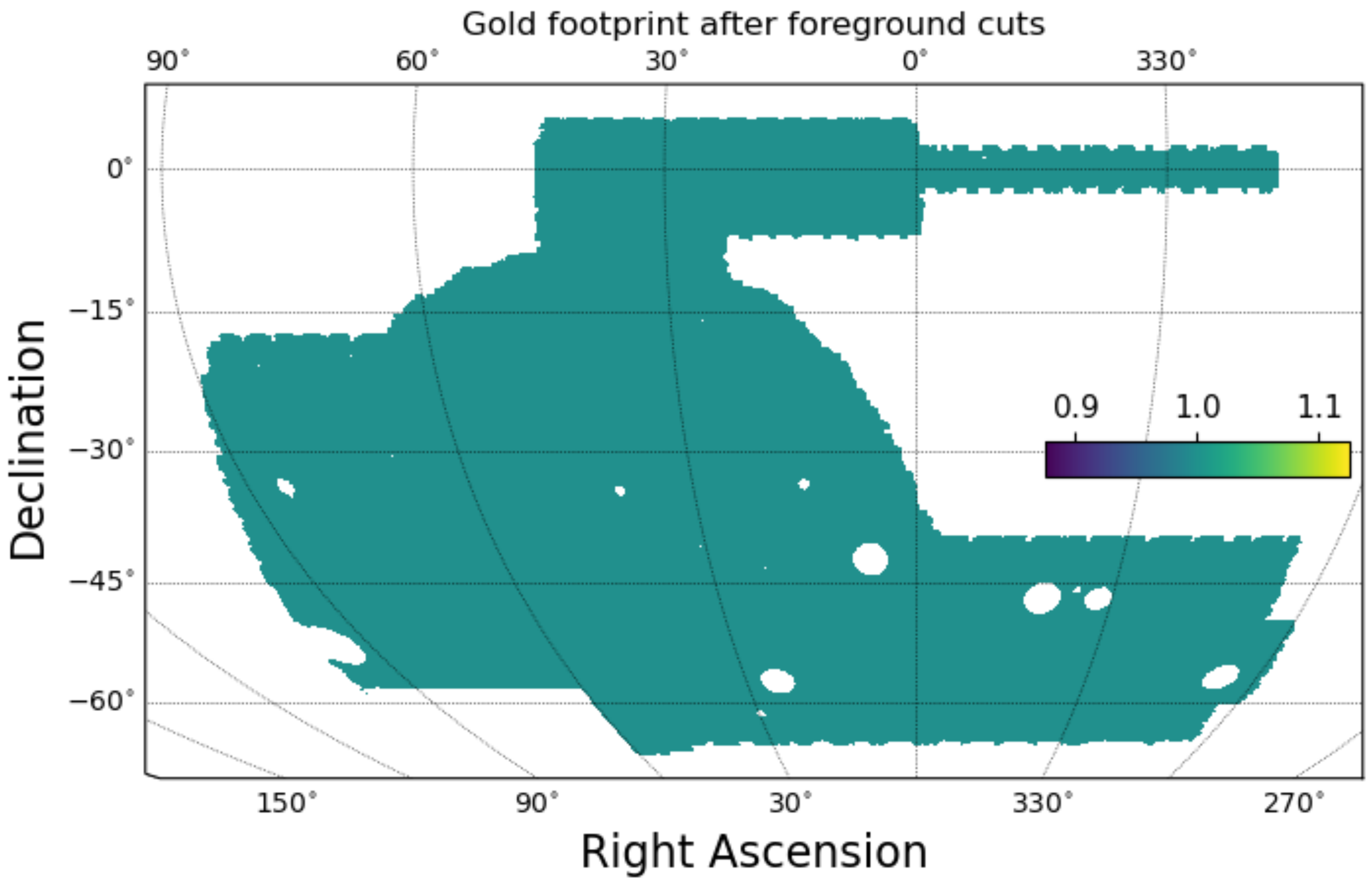

Conclusions

- Using DES Y3 data, we apply the 3D correlation function to measure the BAO on a red galaxy sample with 7 million galaxies in the redshift range of [0.6,1.1] over a field of 4180 deg^2.

- Modeling includes general photo-z distribution and more robust Gaussian window function is considered

- We find $D_\mathrm{M}/r_\mathrm{d} = 19.15 \pm 0.58$ (Gaussian) and $D_\mathrm{M}/r_\mathrm{d} = 19.00 \pm 0.67$ (Top-hat). The constraint is weaker than w b/c the sample is heterogeneous in BAO signals and for the combo 2-4 bins, the constraint from ξ_p is indeed stronger

- The deviation from Planck is reduced from 2.5 sigma to 1.6 sigma.

- ξ_p is complementary to the angular statistics, serve as useful crosscheck, one of the fiducial statistics in Y6 BAO analysis